

Subsea compression Gullfaks Sør satellite field

EiT - Gullfaks village 2013



NTNU
Norwegian University of
Science and Technology



Group 1

Teyyub Amirbayov, Juan Carlos Gloria Lopez, Dicky Harishidayat, Ailo Aasen, Ole Christian Auran
and Malin Kristina Salmi Stavrum

05/02/2013

Abstract

To achieve a higher gas recovery from the Gullfaks Sør field, Statoil has planned to implement subsea compression in the Gullfaks Sør field in October 2015. The project focus was to find a simple way to model this, and to evaluate the effect of the subsea compressor on the net present value (NPV). We considered two subsea production templates (L- and M-template), both during pre-compression and after installation. We try to determine the value of the compressor by comparing the NPVs in different scenarios, with and without subsea compression. In addition to subsea compression, we have evaluated different strategies of enhancing production, like optimizing the production strategy and doing low-pressure separation. In addition, we have tried to model the compressor and validate its characteristics, and also done some flow assurance related to hydrate formation.

Preface

This report is written as part of TPG 4851 Experts in Team, Gullfaks Village spring 2013, in cooperation with the Statoil Gullfaks license in Bergen. The goal of this village has been to review new ways to increase the gas recovery from the satellite field, Gullfaks Sør by installing new subsea equipment or other modifications.

We would like to thank the village supervisors Professor Michael Golan, Professor Jon Kleppe, PhD students Milan Edvard Wolf Stanko, Mayembe Joao Bartolome and Jesus Alberto De Andrade Correia, and associate professor Jan Ivar Jensen for helpful guidance throughout the project.

We would also like to thank the project supervisor Hallstein M. Ånesand and Petter Eltvik in Statoil.

Trondheim, May 2013

Teyyub Amirbayov,

Ailo Aasen

Juan Carlos Glora Lopez

Ole Christian Auran

Dicky Harishidayat

Malin Kristina Salmi Stavrum

Table of Contents

Abstract.....	1
Preface.....	2
1. Introduction.....	4
2. Part A.....	7
2.1 Method of execution.....	7
2.2 Results and discussion.....	8
2.2.1 Compressor map.....	11
3. Part B.....	12
3.1 Material balance calculations based on black oil properties.....	12
3.1.1 Results from IPT- Material balance.....	16
3.2 Wet gas compression.....	19
3.2.1 Compressor validation.....	19
3.2.2 Wet gas compressors in parallel.....	21
3.2.3 Wet gas compressors in series.....	21
3.3 Flow assurance, hydrate formation.....	22
3.3.1 14” Pipeline.....	24
3.3.2 8” pipeline.....	24
3.4 Production management in different scenarios.....	25
3.4.1 Modifying the Excel model from part A.....	26
3.4.2 Scenario 1B: Shutting down one of the pipes in 2015.....	27
3.4.1 Scenario 2B: The best case - finding an optimal production strategy.....	27
4. Economical calculations.....	31
4.1 General economy.....	31
4.2 Evaluating the NPV of the compressor project in different scenarios.....	33
4.2 Evaluating the production management scenarios.....	35
5. Summary and recommendations.....	37
List of Symbols, abbreviation and Quantities used.....	38
Literature.....	39
List of appendix.....	40

1. Introduction

The Gullfaks field started producing oil and gas December 1986. After the discovery in 1978, the field was assigned to three Norwegian companies: Statoil, Norsk Hydro and Saga Petroleum, with Statoil as the operator. Since production-start, Statoil has used new technologies, such as horizontal and long-ranged wells and alternating water and gas injections to achieve a high recovery for oil and gas from the field. The recovery factor of Gullfaks today is estimated to be 59 %, but the goal is increasing it to 62%. Increasing the oil and gas recovery is the key concept for the Gullfaks Village.

The Gullfaks field lies in block 34/10 of the northern part of the North Sea. The main field has three production platforms (A, B and C) with concrete substructure. The satellite fields Gullfaks Sør, Rimfaks, Skinfaks og Gullveig has been developed with subsea wells which are remotely operated from Gullfaks A and C platforms. The Gullfaks field is illustrated in figure 1. [1]

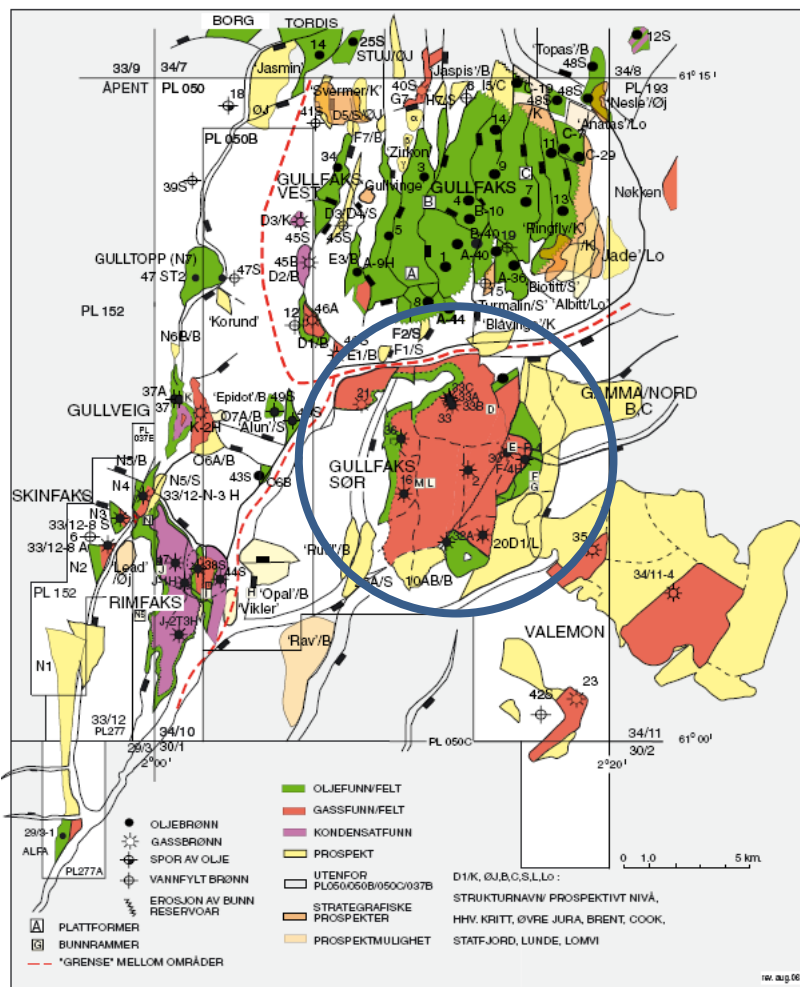


Figure 1 Map of Gullfaks area. The subsea satellite Gullfaks Sør field is shown in the blue circle, to the south of the Gullfaks main field. [2]

The object for this project was to boost and sustain gas and condensate production from the Gullfaks Sør subsea satellite field for template L and M. The L and M templates are illustrated in the Gullfaks

field layout in figure 2. Gullfaks Sør lies in the blocks 34/10 and 33/12, and the water depth of the satellite area is in the range from 130- to 220 meter. Gas from the L- and M field is transported by 2*14" pipeline of 14 km length to Gullfaks C. On the platform the gas is treated and then further transported by pipeline to Kårstø, Stavanger. The gas produced from the Gullfaks Sør field contains condensate which makes the gas more valuable. [3]

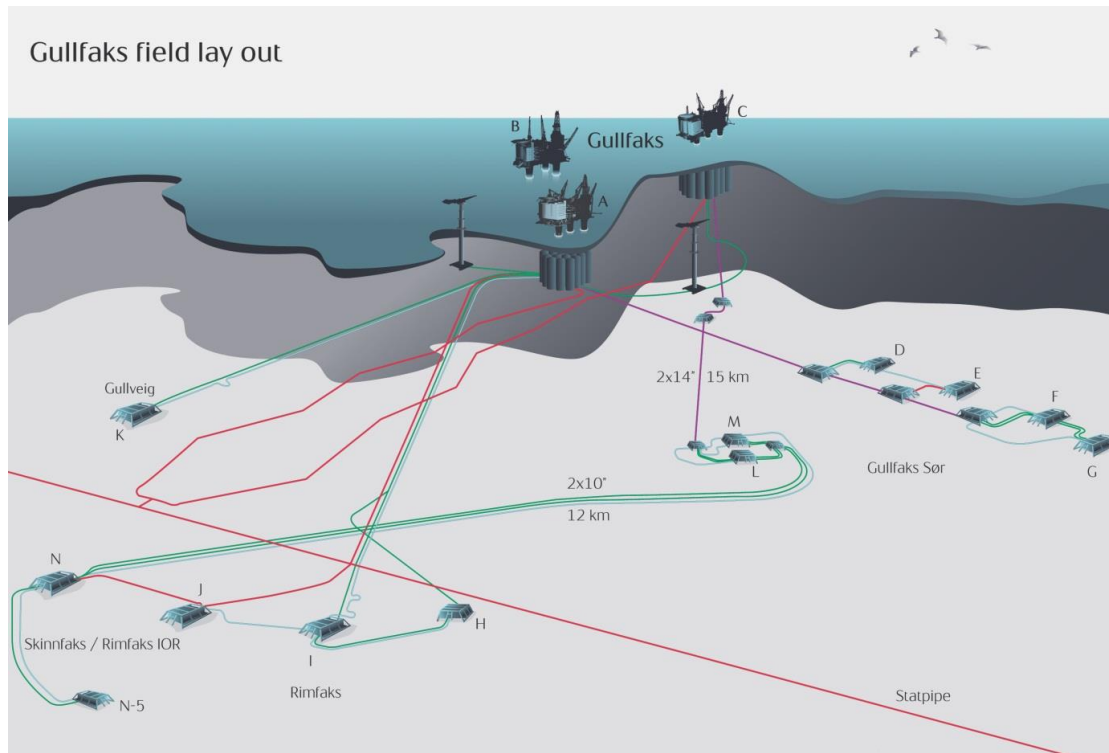


Figure 2 Layout for the satellites fields Gullfaks Sør, Gullveig, Rimfaks and Skinnfaks. [4]

To achieve a higher gas recovery factor from the Gullfaks Sør field, Statoil is installing a multi-phase subsea compressor which is planned to start in 2015. The technology of a multi-phase compressor makes it possible for increased boosting of gas containing condensate and water, which earlier had to be removed upstream in conventional compressors. [5]

Statoil has estimated that the reservoir pressure in the Gullfaks Sør field is reduced to its limit to obtain the 10 MSm³/day plateau in 2015, and therefore the compression is essential to keep the plateau production. The wet gas compression combined with low-pressure modification (LPM) in a later phase can increase the recovery factor from the Gullfaks field from 62% to 74%. Low-pressure modification means reducing the separator pressure of the first stage separator at the platform. [6]

The implementation of the wet gas compressor is estimated to give an extra 22 million barrels and 3 billion standard cubic meter gas from the Gullfaks Sør Brent reservoir. Statoil has invested approximately 3 billion NOK in the wet gas compressor project at the Gullfaks Sør field. [6]

A sketch of the L- and M template with the multi-phase compressor system is illustrated in figure 3.

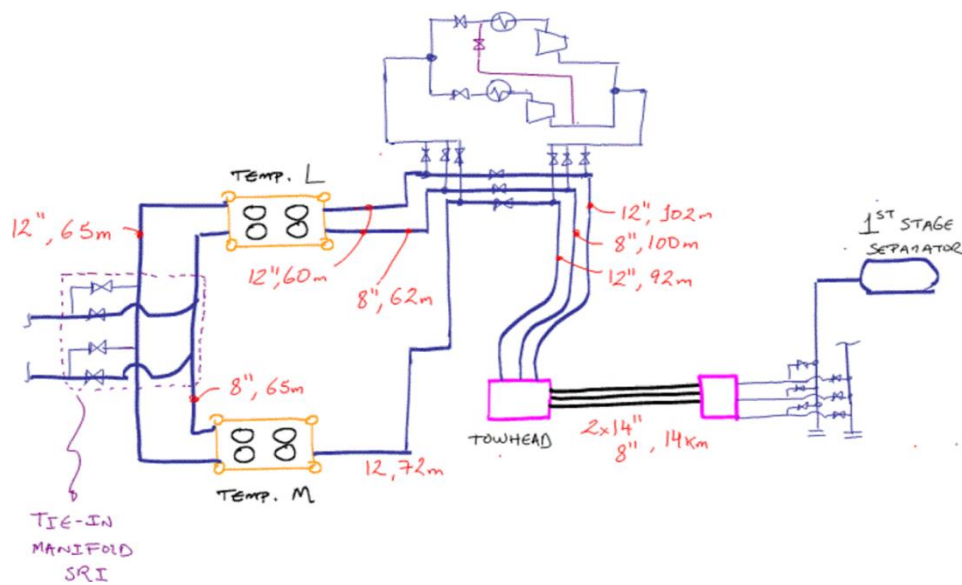


Figure 3 Template L and M. Sketch courtesy of technical supervisor Michael Golan. [7]

The M- template is only operating three wells and not four as shown in figure 3.

The project was divided in two tasks, A and B. In part A, a simple dry gas model was made in excel to try to extend the natural plateau of 10 MSm³/day as long as possible.

In part B several cases were studied. First of all a material balance excel sheet provided made by PhD Milan Stanko was used to see if the assumptions used in part A could be used for the wet gas model. The compressor arrangement was studied to see if the compressors were to run in parallel or in series, and at what time this should happen. A simple wet gas compressor model was made in HYSYS, low pressure modification was used to prolong the plateau. Since the overall goal of the Gullfaks village is to increase the recovery factor and value of the Gullfaks field, this motivates the flow optimization we have done, where we utilize all the value-enhancing technology (e.g. the compressor) at our disposal, and come up with an optimal production strategy. This was time-consuming work, but fortunately it has a conclusion that is easy to understand.

2. Part A

In part A, a model was established in Excel, using the following main assumptions:

- Dry gas only
- Isothermal equations valid
- Only horizontal flow from templates to platform, neglecting vertical pressure loss in riser
- Project start: January 1st 2009
- Project ends when production goes below 5 MSm³/day
- Used two 14” pipes after towhead, 8” not used
- No low-pressure modification
- All 7 wells are identical
- Wells in the same template have the same wellhead pressure

Also a simulation was run; we will refer to this as Scenario A. The economic analysis is done in part B, section 4.

2.1 Method of execution

After being presented the relevant data for template L and M (appendix 1) and a simplified set of governing equations (1-4), an excel model was made. The excel sheet made in part A is presented in appendix 2.

Material balance to calculate reservoir pressure:

$$p_R = p_i \left(\frac{z_R}{z_i} \right) \left(1 - \frac{G_p}{G} \right) \quad (1)$$

Pressure in horizontal pipeline:

$$q = C_{FL} (p_{in}^2 - p_{out}^2)^{0.5} \quad (2)$$

Tubing equation:

$$q = C_T \left(\frac{p_{in}^2}{e^s} - p_{out}^2 \right)^{0.5} \quad (3)$$

Inflow equation reservoir to wellfloor

$$q = C_R (p_R^2 - p_{wf}^2)^n \quad (4)$$

where p_R is reservoir pressure, p_i the initial pressure, z_R, z_i are compressibility factors, G is the gas initially in place, G_p is the gas produced, C_{FL} is the pre-compression spool coefficient, C_T is the Tubing coefficient, C_R the Reservoir coefficient, p_{wf} is the wellfloor pressure.

The production period is divided into three stages. The first period is the natural plateau, with constant total flow rate of $10\text{MSm}^3/\text{day}$. In this period the reservoir pressure is high enough that compression is not needed. The second stage is the compression plateau. As the reservoir pressure drops to the point where it is not able to get $10\text{MSm}^3/\text{day}$, the compressor is started, allowing to prolong the plateau while still producing $10\text{MSm}^3/\text{day}$. In the third stage the total production of $10\text{MSm}^3/\text{day}$ is reduced. The differential pressure of the compressor is limited to 32 bara, which means that after this limit is reached the flow rate has to be decreased to avoid overloading of the compressor. The production is continued until the flow rate reaches $5\text{MSm}^3/\text{day}$.

We give an outline of how the simulation was done; it all boils down to pressure calculations. During the years of the natural plateau, we adjust the rates from the two templates by using chokes stationed at the wellheads¹. Knowing the GIP and the G_p we know the reservoir pressure. Knowing the production rates allows us to calculate the pressure at the wellheads using equation (3). Equation (4) gives us the pressure at the towhead, and then finally at the platform², which needs to be above 65 bara because of the separator. When the compressor is installed, the main difference is that we can no longer control the rates ourselves since the chokes by this time already are fully opened. We therefore have to solve for the rates from the two templates using that the flows are mixed before the compressor, and therefore have the same pressure at its intake. The plateau is sustained until the differential pressure over the compressor reaches 32 bar; at that point the differential pressure is fixed, and we let the production decline until it reaches $5\text{MSm}^3/\text{day}$.

The Excel solver was needed for pressure calculations from the compression plateau and till the end of production.

A compressor chart made in excel is also presented. This was made to check if the compressor will be able to perform in the actual operating conditions.

2.2 Results and discussion

Flow rates q , for template L-east and M-west, were manipulated manually in excel to extend the natural plateau with a total flow rate of $10\text{MSm}^3/\text{day}$ for as long as possible. The results of the production period are given in table 1.

¹ In later simulations we have placed the choke on the platform instead.

²This is where we use the assumption of no vertical pressure loss due to the elevation of the platform

Table 1 Results of the end of natural-, compression plateau and production.

End of:	Year
Natural plateau	June 2016
Compression plateau	July 2018
Production	January 2025

Figure 4 illustrates the flow rate for template L and M during the production period from 2009 to 2025. Figure 5 and 6 illustrates the pressures for the well-head, well flow, reservoir, separator, towhead and template during the production period for template L and M respectively. In these figures the choke is the difference between p_{wh} and $P_{template}$. The graph for $P_{template}$ lies underneath $P_{towhead}$, since the pressure loss from the template to the towhead is negligible.

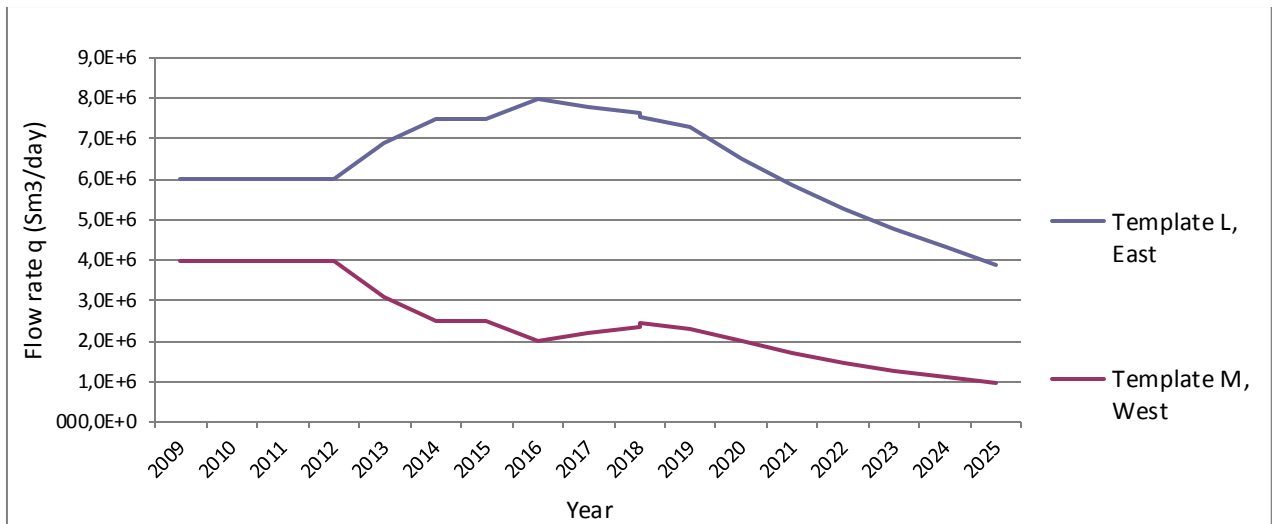


Figure 4 Flow rate of template L and M versus time in production period

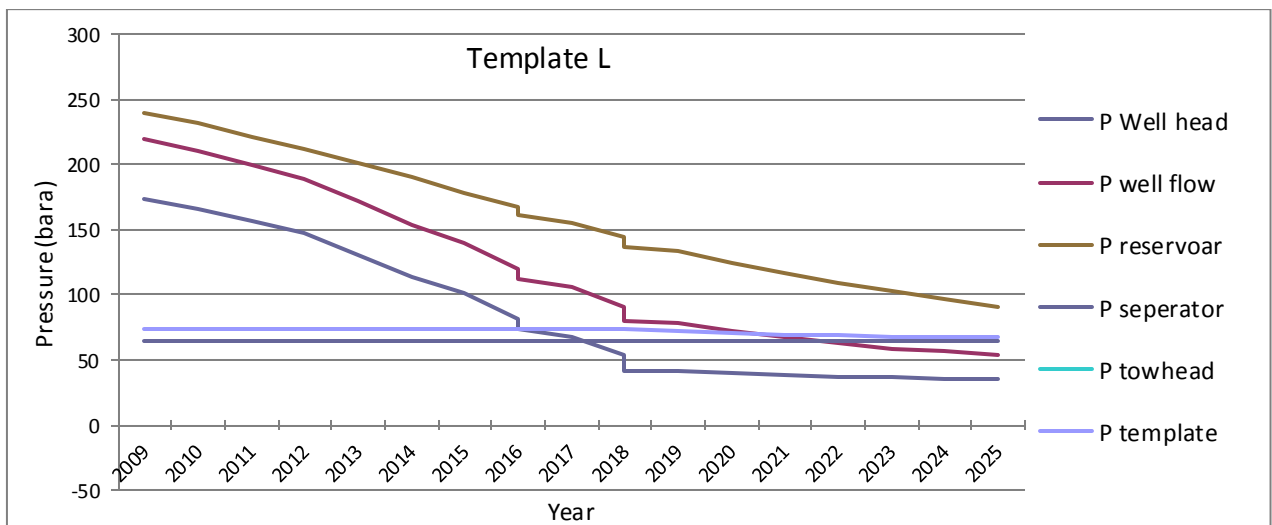


Figure 5 Well head-, well flow-, reservoir-, separator-, towhead- and template pressure for template-L versus time.

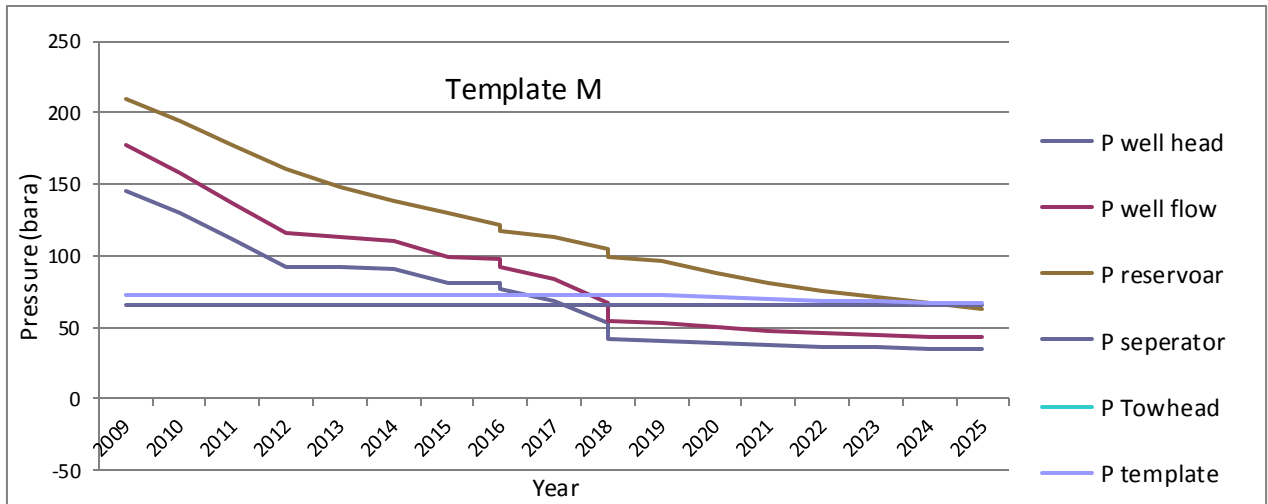


Figure 6 Well head-, well flow-, reservoir-, separator-, towhead- and template pressure for template M versus time.

The total decreasing production flow rate is illustrated in figure 7.

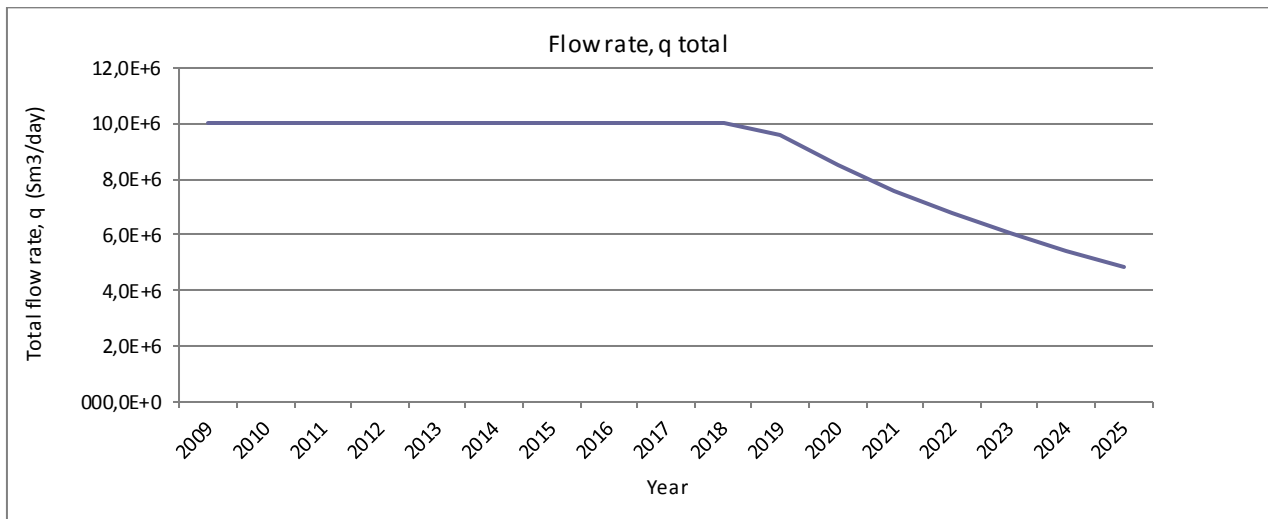


Figure 7 The total flow rate for template M and L in between year 2008 - 2024.

As can be seen in Figure 4, during the natural plateau we increased the production from L and decreased production from M. This is related to the fact that the GIIP for the two reservoirs differ by a factor of 3.

In figure 5 and 6, we give an overview of how the pressures at some stages in the transport of the gas from the reservoir on its way to the platform.

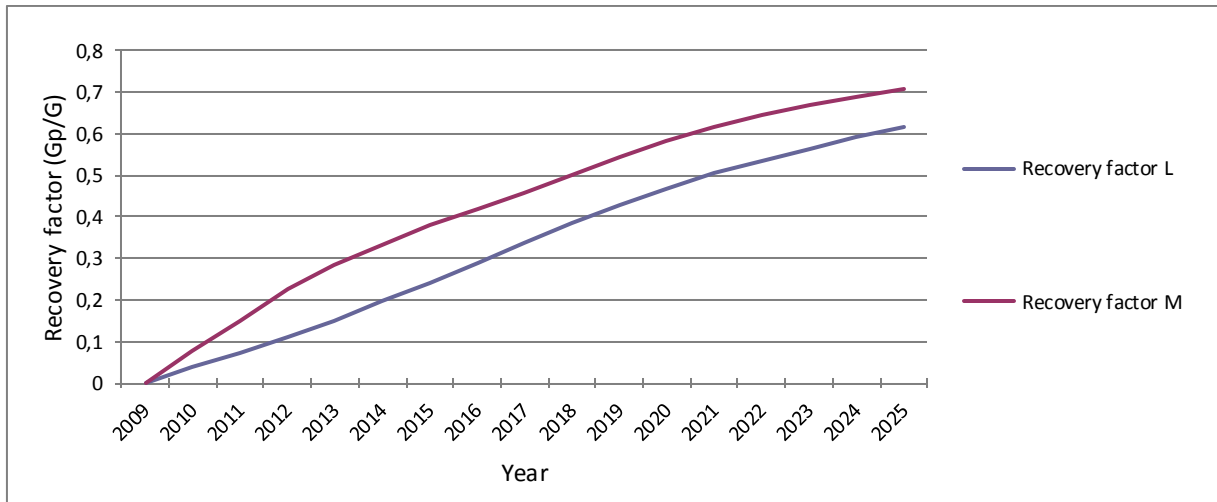


Figure 8 Recovery factor for template L and M

The recovery factors for field L and M at the end of production, can be viewed in figure 8, and were determined to be 0.61 and 0.71 respectively.

2.2.1 Compressor map

After running tests on the compressor, Framo Engineering claims the compressor has no operational constraints related to Surge (minimum flow rate), stone wall (maximum flow rate), or mechanical issues. No information have been given on minimal suction pressure of the compressor, this is therefore not included as a constraint. Constraints related to the compressor are as follows:

- Compressor speed: $N = (2000-4500)$ rpm. A recommendation from Framo Engineering.
- Discharge temperature: $T_d < 110^\circ\text{C}$. This limitation is related to buckling of the pipe.
- Minimum inlet temperature is set to 35°C .
- Power consumption of each compressor is set to a maximum of 5MW.
- Maximum pressure increase over one compressor (ΔP) is 32 bar.
- Maximum pressure increase over both compressors is 60 bar
- Maximum flow capacity of each compressor is $6000 \text{ m}^3/\text{h}$.

Results from the compressor map is based on the flow rates and pressures from the excel file (appendix 1). One compressor map was made for each year. For each year the compressors were set in parallel and in series. Variables changing during the test were suction pressure, discharge pressure and inlet flow. The inlet temperature was fixed at 35°C . The compressor maps are illustrated in appendix 3.

The results shows that from 2016-2021 the flow is too big for one single compressor to handle, so the compressors need to be arranged in parallel. From 2021 the flow is reduced a lot, so now the main parameter is the pressure ratio of the compressors. If the compressors are kept in parallel, the limitation of the pressure ratio is exceeded. Therefore the arrangement is changed to series from 2021. This will fix the compressor ratio, and also manage the total flow rate.

3. Part B

In part A the main production model was established, a technical overview of the compressor characteristics was given and Scenario A with no LPM was simulated. In part B, the dry gas assumption was validated from part A, and the dry gas model was expanded to include condensate. Further a thorough validation of the compressor characteristics was performed. Two new production scenarios were treated. In the first, scenario 1B, the production is subject to restrictions on what pipes which can be used to transport the gas from the templates to the platform. In the second scenario, 2B, there are no restrictions, and in addition the production strategy for the templates was optimized. Scenario 2B is the best-case scenario, and the production strategy developed is of interest in its own right.

The economic analysis has two main objectives: One is to evaluate the NPV of the compression project in each of the three scenarios. The second is to give the total NPV for each of the simulated cases, showing how the conditions/assumptions on the production affect the total value of the project.

The report is concluded with a summary of conclusions and recommendations.

3.1 Material balance calculations based on black oil properties

In part A of the project one of our main assumptions was a dry gas model, and condensate was not considered. To evaluate this assumption a modified black oil formulation was used instead of traditional formulation.

In order to calculate the amount of condensate produced from Gullfaks C, certain properties from the condensate produced is needed. To generate these properties, HYSYS was used. Composition of the gas- condensate in the reservoir was provided by Statoil, and can be viewed in the appendix 4. The following equations and steps show the foundation of the calculations, and are included to give a general overview of the method. Calculations done for oil from reservoir gas are taken into account and the complete calculation method used can be viewed in appendix(4). It is important to specify that the calculation method was implemented in a Excel sheet called Material Balance (MATBAL) made by PhD Milan Stanko at NTNU, and that this sheet simply was used to generate the black oil parameters by changing reservoir pressure using HYSYS. The calculations are based on the Whitson balance.[8]

For the traditional BO formulation three properties is used to relate surface and reservoir volumes, shown in equations 5-7:

$$R_s = \frac{\text{volume of surface gas dissolved in reservoir oil}}{\text{volume of stock-tank oil from reservoir oil}} \quad (5)$$

$$B_o = \frac{\text{volume of reservoir oil}}{\text{volume of stock-tank oil from reservoir oil}} \quad (6)$$

$$B_g = \frac{\text{volume of reservoir gas}}{\text{volume of surface gas from reservoir gas}} \quad (7)$$

“These three properties constitute the traditional black-oil PVT formulation, which has the following assumptions:

1. Reservoir oil consists of two surface “components,” stock-tank oil and surface total separator gas.
2. Reservoir gas does not yield liquids when brought to the surface.
3. Surface gas released from the reservoir oil has the same properties as the reservoir gas.
4. Properties of stock-tank oil and surface gas do not change during depletion of a reservoir.”

The modified Black Oil model includes an oil condensate, while still being simpler than solving a problem using component by component basis. The four Modified Black Oil(MBO) PVT parameters, oil formation volume factor (B_o) , solution gas-oil ratio (R_s), dry gas formation volume factor (B_{gd}), solution oil-gas ratio (r_s) are defined as

$$B_o = \frac{V_o}{V_{\bar{o}o}} \quad (8)$$

$$R_s = \frac{V_{go}}{V_{\bar{o}o}} \quad (9)$$

$$B_{gd} = \frac{V_g}{V_{\bar{g}g}} \quad (10)$$

$$r_s = \frac{V_{og}}{V_{\bar{g}g}} \quad (11)$$

Where,

V_o – reservoir-oil volume,

$V_{\bar{o}o}$ – volume of stock-tank oil produced from the reservoir oil,

$V_{\bar{g}o}$ – volume of surface gas produced from the reservoir oil,

V_g – reservoir gas volume,

$V_{\bar{g}g}$ – volume of surface gas produced from the reservoir gas,

$V_{\bar{o}g}$ – stock-tank oil (condensate) produced from the reservoir gas.

From these definitions, a spreadsheet in HYSYS was made, and implemented further on in IPT-Material balance. Table 2 shows the values generated in HYSYS, for different pressures. The simulation was performed in steady state, so the pressures were changed manually for each pressure step. μ_{o} and μ_{g} is the viscosity of the reservoir oil and reservoir gas respectively. Also densities for each material stream is provided; ρ_{og} , ρ_{oo} , ρ_{go} and ρ_{gg} . γ_{ao} and γ_{ag} is defined as:

$$\gamma_{ao} = \frac{\rho_{og}}{\rho_{oo}} \quad (12)$$

$$\gamma_{ag} = \frac{\rho_{go}}{\rho_{gg}} \quad (13)$$

Table 2 Black oil properties from HYSYS.

p	B _o	B _g	R _s	r _s	mu	mu _g	deno	deno	gamma	deng	deng	gamma
bar	m ³ /Sm	m ³ /Sm	Sm ³ /Sm	Sm ³ /Sm	cp	cp	Kg/m ³	Kg/m	-	Kg/m	Kg/m	-
a	³	³	³	³				³		³	³	
240	1,656	0,006	187,96	1,02E-04	0,193	2,27E-02	793,430	802,62	0,989	0,890	0,821	1,084
220	1,591	0,006	164,44	8,16E-05	0,209	2,15E-02	793,065	802,26	0,989	0,897	0,822	1,092
200	1,533	0,007	143,04	6,46E-05	0,224	2,05E-02	792,94	801,89	0,989	0,905	0,823	1,100
180	1,478	0,007	123,40	5,05E-05	0,241	1,96E-02	793,03	801,52	0,989	0,914	0,824	1,109
160	1,425	0,008	105,22	3,92E-05	0,258	1,87E-02	793,23	801,17	0,990	0,923	0,825	1,119
140	1,375	0,009	88,29	3,04E-05	0,277	1,79E-02	793,30	800,90	0,991	0,932	0,825	1,130
120	1,327	0,011	72,47	2,40E-05	0,297	1,72E-02	792,94	800,75	0,990	0,942	0,825	1,141
100	1,281	0,013	57,63	1,95E-05	0,319	1,66E-02	791,85	800,81	0,989	0,951	0,825	1,153
80	1,239	0,016	43,74	1,69E-05	0,343	1,60E-02	789,87	801,21	0,986	0,961	0,826	1,163
60	1,200	0,022	30,69	1,58E-05	0,372	1,55E-02	787,46	802,09	0,982	0,964	0,827	1,165

3.1.1 Results from IPT- Material balance

In the following section results from the MATBAL is shown. In MATBAL a comparison between dry gas and wet gas can be plotted, and the difference can therefore be analyzed. Results from MATBAL was further on implemented in the economic analysis to evaluate the condensate produced.

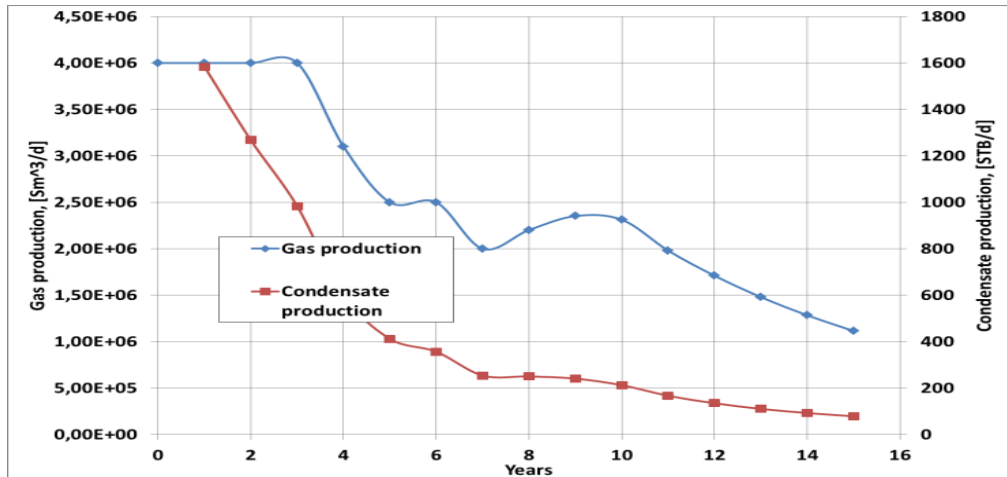


Figure 9: Gas condensate and dry gas production vs time for template L

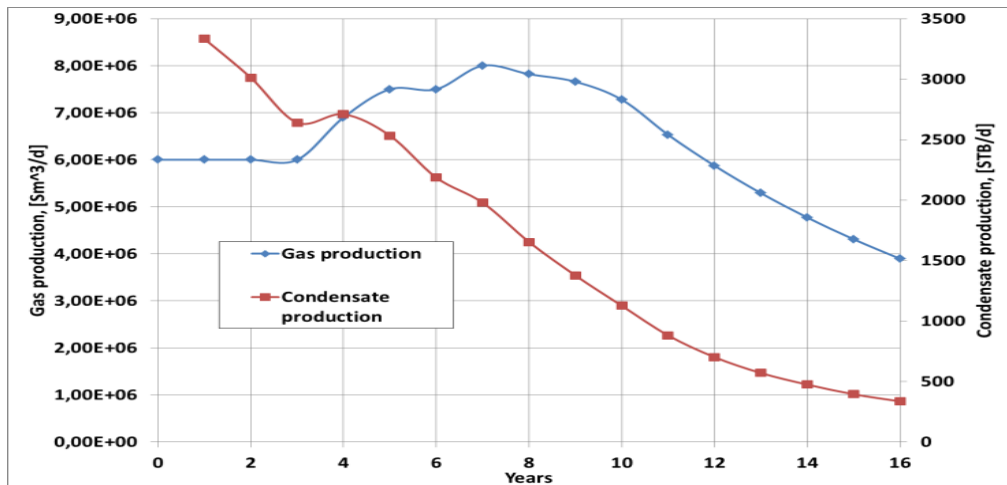


Figure 10: Gas condensate and dry gas production vs time for template M

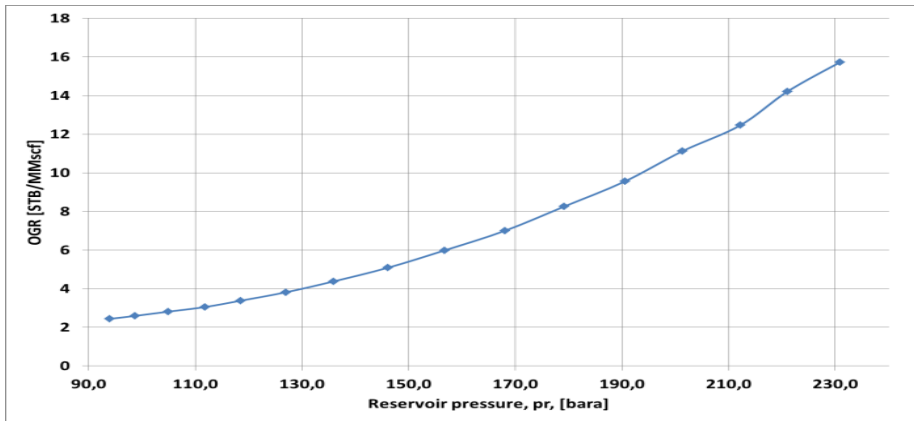


Figure 11: Oil-Gas Ratio vs Reservoir pressure for template L

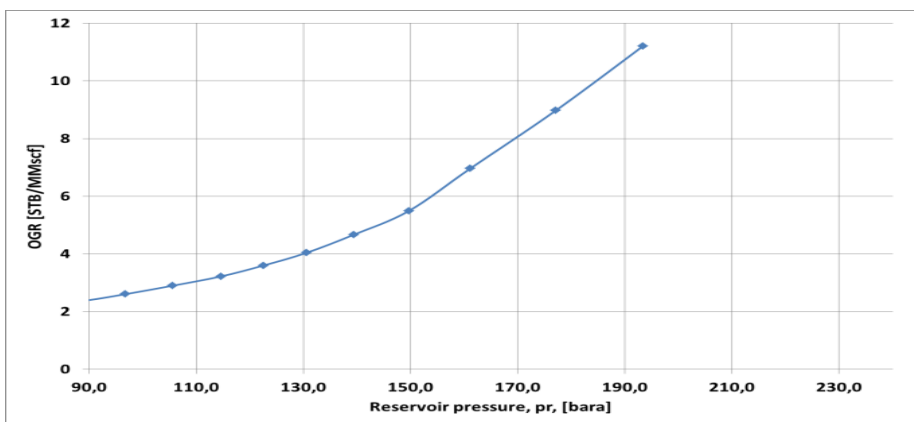


Figure 12: Oil-Gas Ratio vs Reservoir pressure for template M

It can be observed from these plots that the oil gas ratio(OGR) decreases with decreasing pressure. At high initial reservoir pressure we experience high oil-gas ratio.

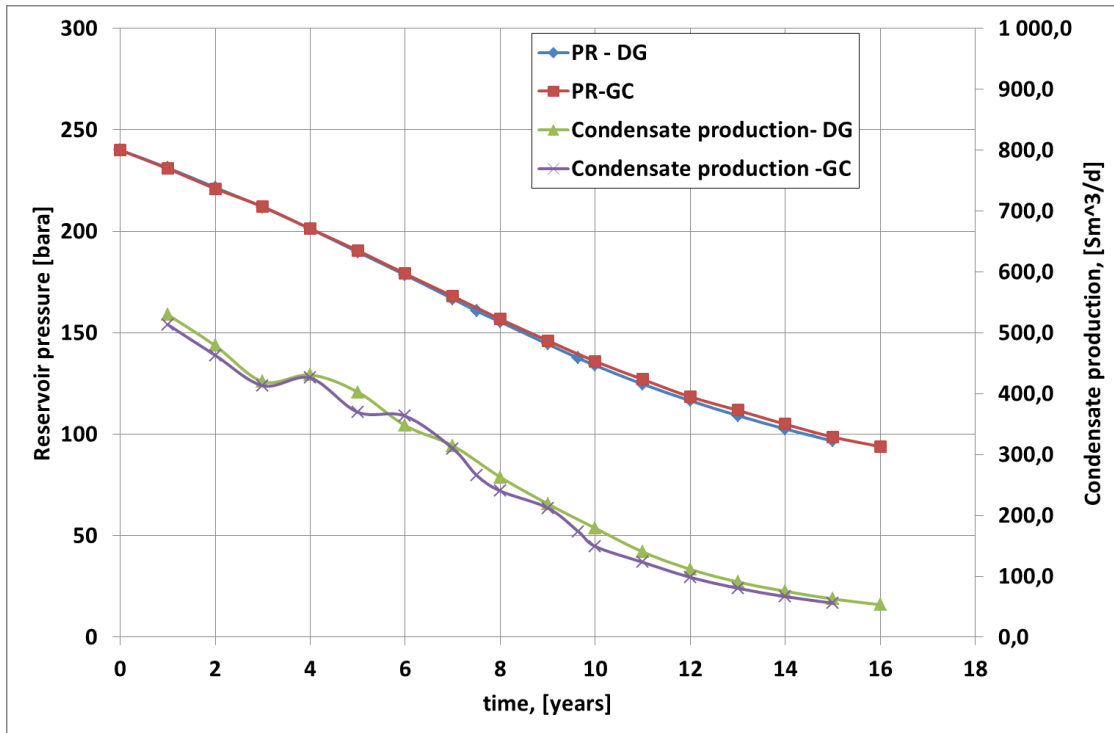


Figure 13: Reservoir pressure and condensate production for template L

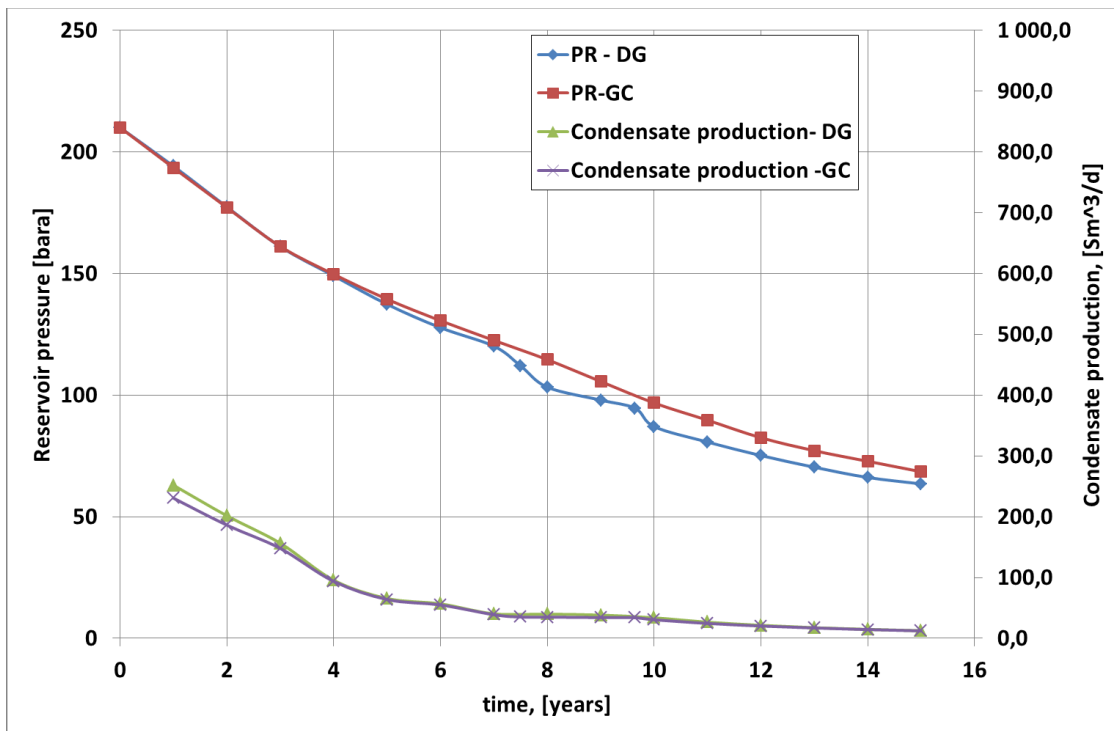


Figure 14: Reservoir pressure and condensate production for template M

In the Part A of the Gullfaks project a dry gas model was one of the main assumptions. In the reality there is some amount of condensate coming out to the surface from the reservoir gas. In our

calculations the main goal was to find out the effect of wet gas and to check whether or not our dry gas assumption was valid.

As shown in the plots there is a slight difference between the gas-condensate and dry gas models, but the difference is so small that it is negligible. Therefore we concluded that our assumption is valid, based on comparison of reservoir pressure and condensate production.

3.2 Wet gas compression

At high pressures and temperatures, the ideal gas behavior is not valid due to changes in fluid properties. Therefore we need a correlation for this. In HYSYS, one option is to choose the Schultz equation. This is a polytropic calculation method which takes into account the real gas behavior. The procedure assumes a polytropic compression path based on averaged gas properties of inlet and outlet conditions.

The presence of liquid increases the flow complexity in the compressor. Fluid properties may vary through the compression process due to energy transfer between the phases. The dry gas performance analysis becomes insufficient when analyzing wet gas compressor performance. A detailed analysis of the fluid properties along the compression path is essential to assure correct calculations. The phase exchange during wet gas compression is not accounted for when utilizing averaged gas properties as in the Schultz procedure.

Another important thing is that the amount of liquid present in the compression process will reduce the discharge temperature of the compressor. [9]

3.2.1 Compressor validation

As of today there exists no method of modeling a multiphase compressor. There are several approaches on how to do it, but no general model implemented in a simulation program. One approach of modeling the subsea process in Gullfaks south is to put a separator upstream the compressor. Here the gas and liquid will be separated into two separated phases. Further on you insert a pump to pump the liquid, and a compressor to compress the gas. The outlet streams of the compressor and the pump get mixed together at the end, and now you can compare the total effect of the compressor and the pump. An arrangement on how this could be done in HYSYS, is illustrated in the figure 15.

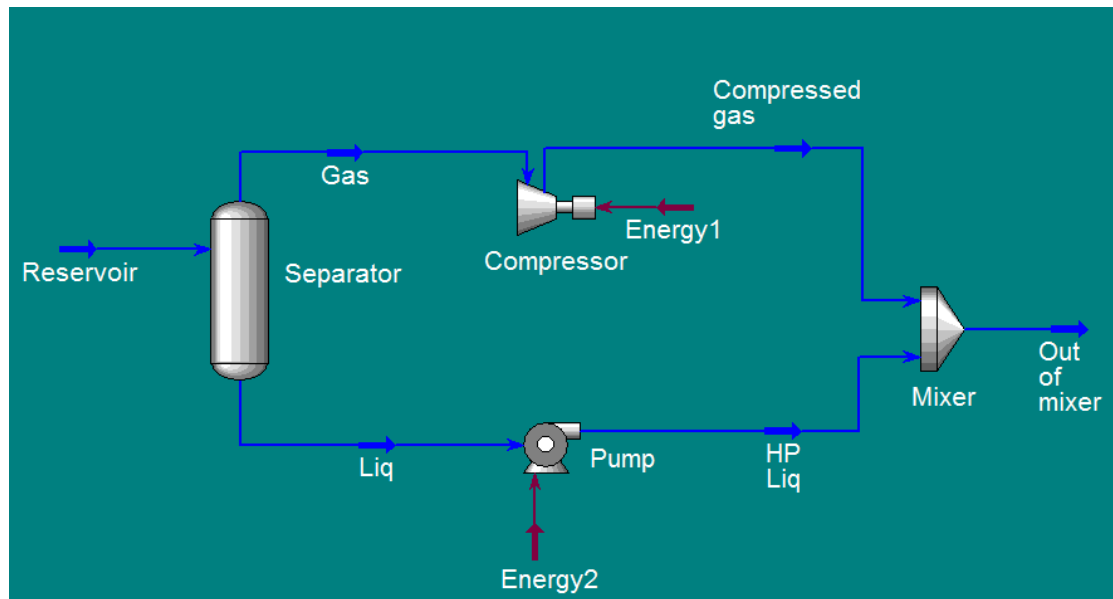


Figure 15 Reservoir stream separated in HYSYS

Another approach is to simulate the compressor in HYSYS as a wet compressor. One of the differences between this approach, and the one mentioned above is that the cooling effect of the liquid will now be present in the simulation.

To validate the compressor characteristics, a comparison with the Excel sheet provided by the Gullfaks Village and a steady state simulation in HYSYS was done. The main goal of this comparison was to check the cooling effect of the liquid in the wet gas, related to the constraint of the discharge temperature of the compressor. Also a comparison of the power consumption was of interest.

The Excel sheet is based on test results from Framo Engineering, and calculates compression based on dry gas behavior. The excel sheet uses ideal gas behavior, and the Z-factor to calculate the output parameters of the compressor. The HYSYS model is based on the reservoir composition given by Statoil, with an initial vapor phase fraction of 0,9619 and a liquid phase fraction of 0,0381. Peng Robinson was used as equation of state.

Temperature of the inlet stream to the compressor was kept constant at 35°C. Suction pressure, discharge pressure and flow rate was changed according to the flow optimization sheet from Excel. For each compressor curve, the polytrophic efficiency was corrected for, by using the excel sheet.

One of the assumptions done in this comparison is that the polytrophic efficiency is the same for the dry gas and the wet gas. Meaning that we neglect the effect the liquid in the wet gas will have on the polytrophic efficiency.

For each simulation, values was taken from HYSYS, and implemented into Excel. From Excel the polytrophic efficiency was taken, and used in HYSYS. Results were then compared. Only the main

results will be mentioned in the following sections. For all results, see appendix(...) Simulation was performed for compressors arranged in parallel and series.

3.2.2 Wet gas compressors in parallel

For the compressor arrangement in parallel, a splitter was inserted to split the reservoir stream in half, giving the compressors the same flow. A picture of the arrangement can be viewed in the figure 16. In the figure the compressors turn yellow because of the liquid content in the gas.

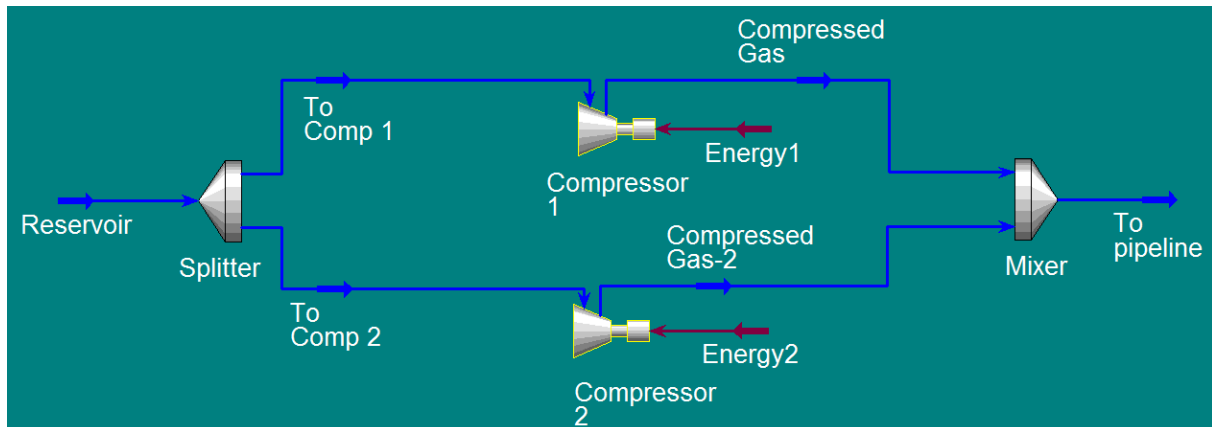


Figure 16 Wet gas compressors in parallel in HYSYS

The two different methods give a large difference in discharge temperature. The discharge temperature from Excel is throughout higher than the discharge temperature from HYSYS. The difference lies between 14-41 %. The main reason for this is due to the cooling effect from the liquid.

The difference in power consumption was fairly small, 2-10%, where the power consumption from the Excel sheet was higher throughout the comparison.

3.2.3 Wet gas compressors in series

In series, the compressors were arranged so that the middle pressure corresponded to the optimum in two- stage compression. This is when the pressure ratios are equal (equation 14-15) [10]

$$\frac{P_2}{P_1} = \frac{P_3}{P_2} \quad (14)$$

Rearranging this equation we get

$$P_2 = \sqrt{P_1 P_3} \quad (15)$$

Where:

P_1 : Suction pressure of first compressor

P_2 : Middle pressure between compressors

P_3 : Discharge of second compressor

Because of limitations for the Excel sheet, only the first compressor in series was evaluated. The simulation in HYSYS is illustrated in figure 17.

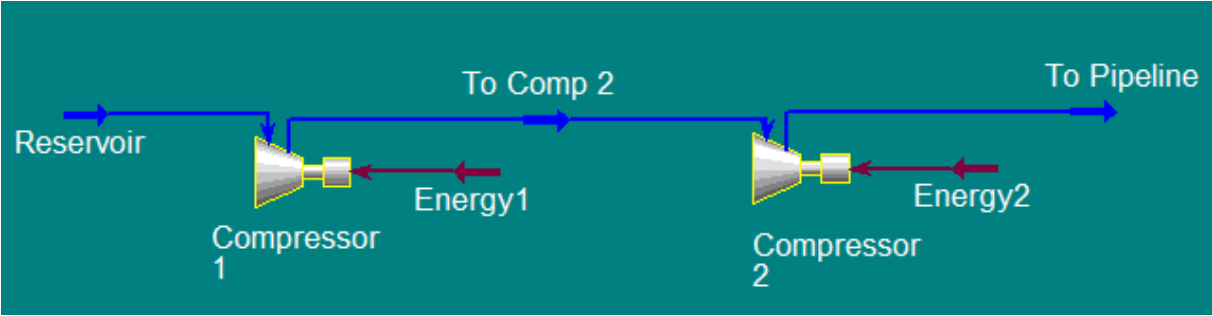


Figure 17 Wet gas compressors in series in HYSYS.

The results show a higher discharge temperature from the Excel sheet compared to the simulation in HYSYS. The difference is between 9-30%. Somewhat a lower difference compared to the parallel simulation, but still significant. Again the cooling effect of the liquid is the main factor why the discharge temperature from HYSYS is lower.

The difference in power consumption was 3-6%, where the power consumption from the Excel sheet was higher throughout the comparison.

3.3 Flow assurance, hydrate formation

As a part of the flow assurance part, hydrate formation was studied. Hydrate formation is a big problem in the oil and gas industry, and therefore a study is a necessary and important part of this project. The task was performed in HYSYS, using Beggs and Brill as a multiphase model. The equation of state used was Peng Robinson. The composition of the gas can be viewed in appendix4. The study was done with a 14” pipe and an 8” pipe. First the gas and the condensate was separated out. Further on the gas was mixed with water until the gas was totally saturated with water. At the end, saturated gas and condensate was mixed together and sent through a 14 km long horizontal pipeline. The HYSYS simulation arrangement is illustrated in figure 18.

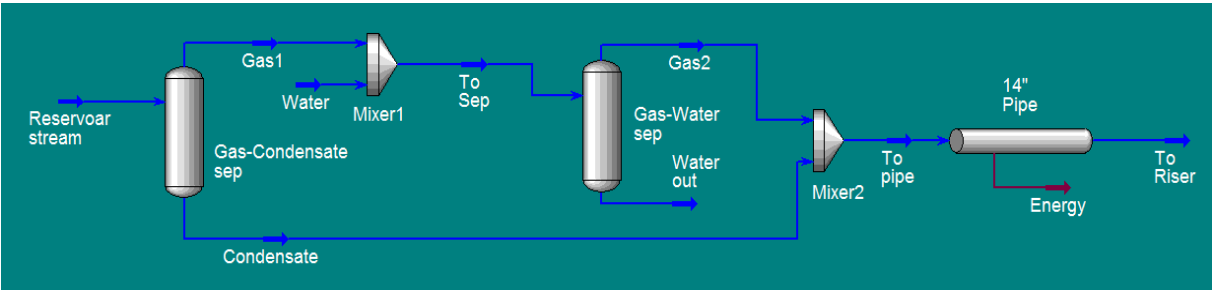


Figure 18 HYSYS simulation arrangement

A phase envelope was made for the reservoir gas, to check the hydrate formation curve. From the curve it can be seen that the hydrate formation temperature is approximately 25°C. This means that hydrates will form if the temperature drops below 25°C, in the 14 km pipeline. The phase envelope taken from HYSYS is illustrated in figure 19.

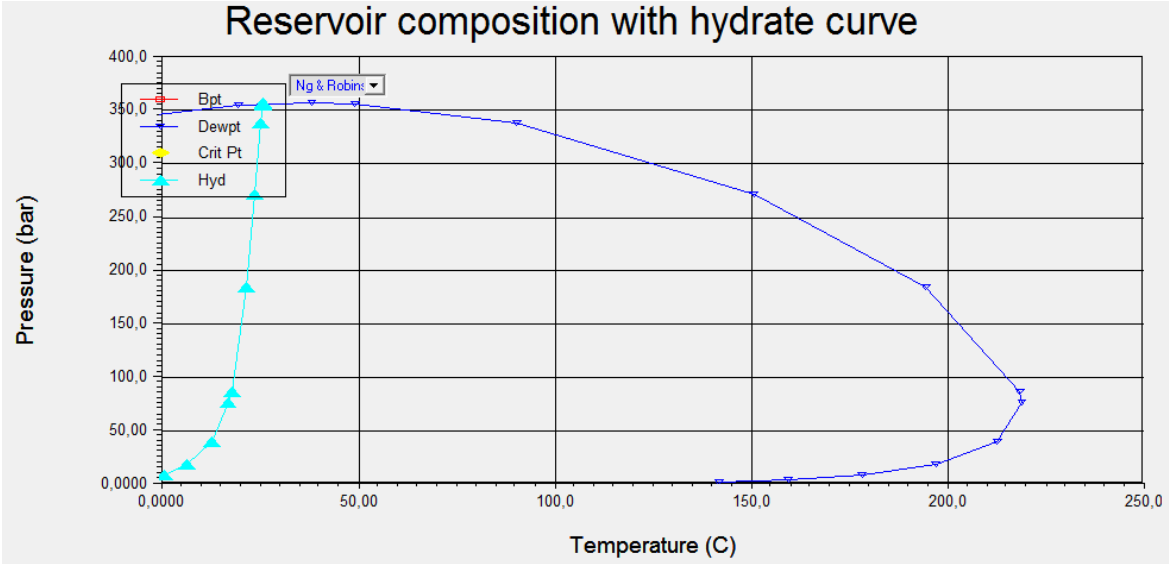


Figure 19 Phase envelope of reservoir gas from HYSYS

In the analysis a constant seabed temperature of 4°C was assumed [9], and also the riser was neglected.

3.3.1 14” Pipeline

The fixed parameters for the 14” pipe is given in table 3. Temperature and pressure of the gas and condensate entering the pipeline was set to 90°C and 73 bara respectively.

Table 3 Fixed parameters of 14” pipe

14” pipe	
Length [km]	14
Elevation change [m]	0
Outer diameter [mm]	355,6
Inner diameter [mm]	320,0
Material	Mild steel
Roughness [m]	4,572e-05
Pipe wall conductivity [W/mK]	45
Overall seawater temperature [°C]	4

During the simulation, sensitivity analysis was done by changing flow rate and overall heat transfer coefficient. The flow rates was taken from the flow optimization part, and varied between 2,5MSm³/d - 5,0MSm³/d. Minimum overall heat transfer coefficient was chosen to be 1,0 W/m²K. A step of 1,0 W/m²K was used in the sensitivity analysis.

From the results of the sensitivity analysis it can be shown that hydrates start forming when the overall heat transfer coefficient is increased to 7.0. This happens when the flow is 2.5MSm³/d, and the temperature out of the pipeline is then 22.89°C.

3.3.2 8” pipeline

The same study was done for the 8” pipeline. The fixed parameters for the 8” pipeline are given in table 4. Temperature and pressure of the gas and condensate entering the pipeline was set to 90°C and 73 bara respectively.

Table 4 Fixed parameters of 8" pipe

8" pipe	
Length [km]	14
Elevation change [m]	0
Outer diameter [mm]	203,2
Inner diameter [mm]	197,0
Material	Mild steel
Roughness [m]	4,572e-05
Pipe wall conductivity [W/mK]	45
Overall seawater temperature [°C]	4

During the simulation, sensitivity analysis was done by changing flow rate and overall heat transfer coefficient. The flow rates was taken from the flow optimization part, and varied between 0,4MSm³/d – 1,4MSm³/d. Minimum overall heat transfer coefficient was chosen to be 0,5 W/m²K. A step of 0,5 W/m²K was used in the sensitivity analysis.

From the results of the sensitivity analysis it can be shown that hydrates start forming when the overall heat transfer coefficient is increased to 2.0. This happens when the flow is 0.4 MSm³/d, and the temperature out of the pipeline is then 23.72°C.

Table 5 Results for both 14" and 8" pipe

	14"	8"
OHTC [W/m ² K]	7	2
Flow rate [MSm ³ /d]	2,5	0,4
Outlet temperature [°C]	22,9	23,7

3.4 Production management in different scenarios

While previous sections have been centered on aspects of our model and technical investigations related to the compressor, the rest of the report will focus on production management. More

specifically, in addition to Scenario A, two more scenarios are simulated with the model. The first one, Scenario 1B, is straightforward to simulate, and only a brief discussion of this scenario is given. Scenario 2B however, is a best-case scenario interesting in its own right, and a detailed description is given.

Each of the three scenarios has two subcases: one with subsea compression and one without, where all of the other conditions (production strategy, LPM or what pipes you are using) are fixed. There are thus six cases in total. Simulating all these cases serves two purposes:

1. One gets the NPV of the compressor project under different operating conditions, giving a more nuanced view of how robust the compressor investment is.
2. One gets the NPV for the total project under different operating conditions, showing the effect of the differences in the cases compared to the project as a whole.

3.4.1 Modifying the Excel model from part A

While the model established in part A is good and outputs realistic numbers, some aspects were changed in part B.

In part A, flows were assumed to mix in the towhead, but it later became clear that there is no mixing³, and the model was changed accordingly. Mixing at the towhead before sending the flow through the 14 km pipes has the benefit of equalizing flows, meaning less pressure loss. Note also that mixing at towhead will automatically make all seven wellhead pressures equal at the end of the natural plateau, as the pressure loss is negligible in the flow lines connecting the templates with the towhead.

In Scenario 1B and 2B the pipes that are used changes, and when compression starts, one has to solve for the flow distribution in the pipes going out of the compressor. Nature will of course arrange itself so as to make the pressures at the end of the pipes equal. If two identical 14" pipes are used, the flow will just split in half. Let's consider the case with one 14". This is the situation in Scenario 1B. Going back to the equation governing pressure loss: $q = C(p_2^2 - p_1^2)^{0,5}$, the flow distribution is found with simple algebra

$$\frac{q_8}{C_8} = (p_2^2 - p_1^2)^{0,5} = \frac{q_{14}}{C_{14}} \Rightarrow q_{14} = \frac{q_{tot}}{1 + \frac{C_8}{C_{14}}} \quad (16)$$

Where q_{tot} is the total flow rate, q_8 is the rate through the 8" etc. Here p_2 will be the separator pressure, while p_1 is the pressure at the compressor outlet. Other situations, for example the case with two 14"s and one 8" as in Scenario 2B, is handled similarly.

³ Statoil/FRAMO staff in Bergen

As previously mentioned, the choke is what makes it possible to control the rates during the natural plateau. The original model in part A assumes subsea choking, but this was later dropped, and the model was changed to implement platform choking. The main difference in the pressure calculations from part A is that to find the pressure difference over the choke, calculations are done upstream instead of downstream. A question that arises is what the effect choking on the platform contra the seabed has. One obvious effect is of course that it raises the pressure of the gas in the pipes on its way to the platform. We haven't investigated what effect this has⁴, but we stress that the placement of the chokes doesn't affect how long one can sustain the natural plateau. This is basically because placing the chokes at the platform and having them fully open, is indistinguishable from placing the chokes at the seabed and having them fully open.⁵

Finally, in Scenario 1B and Scenario 2B, low-pressure modification (LPM) is used. Compression is a way to add pressure energy to the flow. Lowering the separator pressure reduces the pressure energy required after transport to the platform. The default high-pressure separation is set to 65 bara, and this is lowered to 25 bara over the period of a year. It is always initialized at the point where the plateau would have otherwise ended. The result of performing low pressure modification is an extension of the natural plateau with a production of 10 MSm³/day.

3.4.2 Scenario 1B: Shutting down one of the pipes in 2015

In this scenario high-pressure gas from the N-template will occupy the pipeline from the M-template in 2015, which means that the gas from the M-template will have to go through the 8" from that point on. Up to that point flows are as usual sent through separate 14" pipes. There will be an economical loss from this when losing a pipe, since this means that more flow has to go through the remaining pipes, increasing pressure loss due to friction. This means that total flow has to be lowered to compensate, and the model verifies this. The simulation shows that the natural plateau can be maintained until compression installation, if we lower the total flow to 9.85MSm³/day at the start of 2015. After compression installation, the production of course goes back up to 10MSm³/day. It may be possible to do some kind of pressure analysis as above, preventing one from doing this slight lowering of the plateau in the months before compressor installation, but this has not been investigated further.

3.4.1 Scenario 2B: The best case - finding an optimal production strategy

The overall goal of the Gullfaks village is to increase the recovery factor and value of the Gullfaks field. This motivates the flow optimization performed, where all the value-enhancing technology (e.g. the compressor) is utilized at our disposal, and come up with an optimal production strategy. To be more specific, the optimization is as given:

⁴ Our chief technical supervisor, Professor Golan, indicated possible effects related to slugging.

⁵ This may be either obvious or unclear. The point is that placement of chokes won't affect the simulation results.

- **Objective:** Maximize the NPV of the project.
- **Assumptions:** The 8” can be used freely; subsea compression is started at the end of the natural plateau; LP-modification is started at the end of the compression plateau.⁶ Production is stopped when the total flow drops to 5 MSm³/day.

In reality, Statoil has already decided on using both subsea compression and LP-modification, and therefore it is interesting to optimize this case.

To optimize production, a good strategy of producing the fields is needed. A critical factor in this respect is pressure loss of the gas between the reservoir and the platform; indeed the whole point of installing the subsea compressor is to add pressure energy to the flow. In doing this, there has been used intuition coming from the equation governing pressure loss in the pipe, $q = C(p_2^2 - p_1^2)^{0.5}$, where q is the flow rate, C is a constant depending on the pipe, and p_1 and p_2 are respectively the initial and final pressure. This is a nonlinear equation, but it is easier to assess the pressure drop $\Delta p = p_2 - p_1$ if we linearize it using that the ratio $\frac{\Delta p}{p_1} \ll 1$ at our scales, to get

$$q^2 = 2C^2 p_1 \Delta p \left(1 + \frac{\Delta p}{2p_1}\right) \Rightarrow \Delta p \simeq \frac{q^2}{2C^2 p_1} \quad (17)$$

From equation 13 it can be seen that the pressure loss goes approximately quadratically with the flow and inversely with the initial pressure.

The goal of the project is to maximize the NPV, and since the time-value of money decreases, a dollar today is better than a dollar tomorrow. Also the gas prices are projected to decline, so one should definitely strive to get out as much gas as possible early on. This reasoning shows that to get a high NPV, it is preferable with a long plateau, and this has been the main focus of the optimization. Sustaining the natural plateau for as long as possible also has other benefits, both since compression in practice costs money, and because it provides extra time to deal with contingencies, for instance start-up problems of the compressor.

What can be read out of the linearized pressure equation is this: to minimize the total pressure loss with a fixed total flow rate, the flow in the flow in the pipes should be equalized. The model shows that the largest pressure drop of the gas on its way to the platform is through the actual wells (the 7” tubing). Since the ratio of the number of wells in the L- and M-templates is 4/3, the most pressure-economical production is to produce from the templates roughly the same ratio, which during the plateau amounts to about 6 MSm³/day from M-template and 4 MSm³/day from the L-template. These are precisely the ”target rates” given in the project description from Statoil. The problem which becomes apparent after studying the results from the part A simulation in the Appendix is that since

⁶ In particular, we don’t optimize the timing of LP-modification.

the M-reservoir is depleted *relatively* faster than the L-reservoir, even if the production starts out with the 4/3-ratio, the production rate from L has to increase to maintain the plateau.

The key point in our optimized strategy is to *not* try to use the 4/3-ratio for the rates throughout the natural plateau. In the early years, when the reservoir pressure is still high, one can choke as one wants and still produce 10 MSm³/day, because the reservoir pressure in our model only depends on how much we have depleted compared to the GIIP. What one should strive for is to have this “pressure-efficient” 4/3-ratio at the *end* of the natural plateau, and it is this criterion that guides us when deciding how to choke.

Using these insights, the best strategy is to completely shut down production from the M-template the first three years (2009-2011), utilizing that the L-reservoir has enough pressure energy to push through 10 MSm³/day by itself in this time period. In the subsequent years of the natural plateau, one should produce as much as one can from the L-template, always choking as little as possible⁷. From our simulation it can be seen that using this strategy, the wellhead pressures for the L-and M-templates are essentially identical at the end of the natural plateau, while it usually differs by as much as 15-20 bars for the other scenarios⁸ we have simulated using the strategy of *starting* with the optimal ratio. From now on this inferior strategy will be referred to as the *default* strategy. These strategies are totally different, and in the figures below we compare how the recovery factor changes over time for the two strategies.

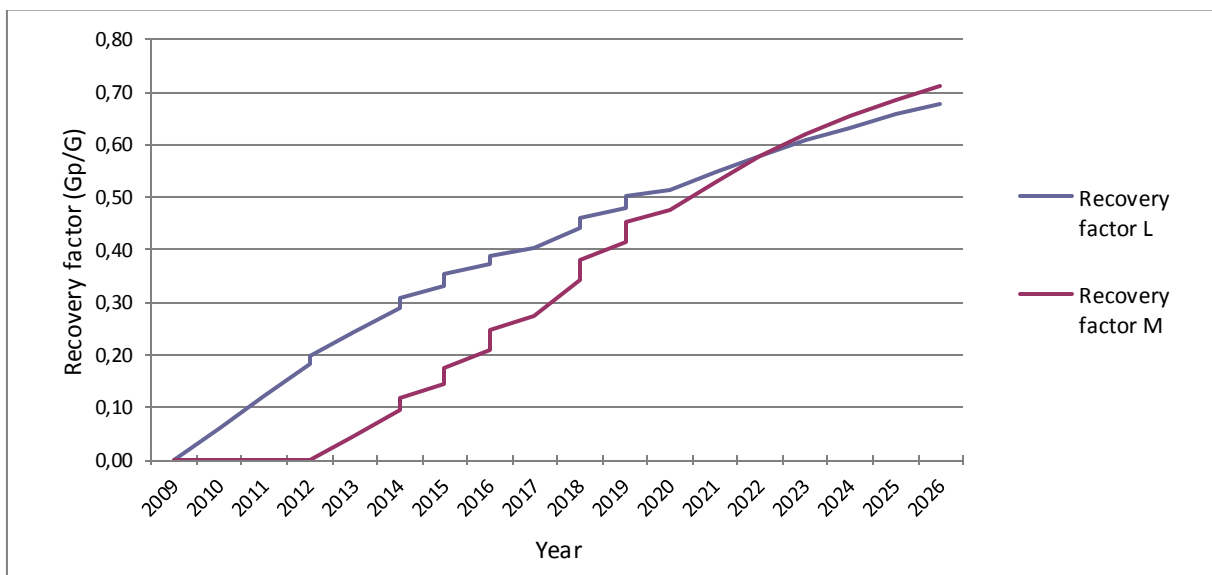


Figure 20: Flow rate for template L and M vs. years with the optimized choking strategy.

⁷ We’ve also assumed that the L-template can’t produce between 7.5 and 10 MSm³/day, since we can’t have flow less than 2.5 MSm³/day through the 14 km transport pipe without aggregation.

⁸ Regrettably, one doesn’t see this in the part A-simulation given in the appendix, because we erroneously mix flows in the towhead.

The recovery factor in this optimized case was determined for L and M to be 68- and 71% respectively.

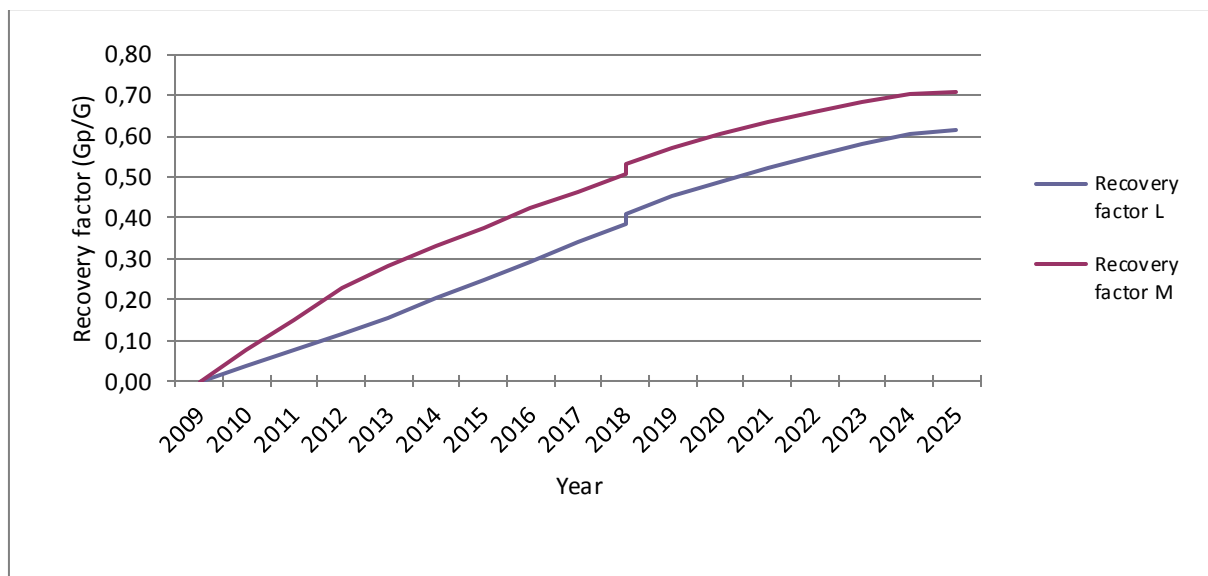


Figure 21: Flow rate for template L and M vs. years with the choking strategy from part A.

The 8” is connected to the L-template at all times, simply because this template is always the one with the highest production rate. Since pressure loss goes approximately as the square of the flow, we expect that we will save more pressure energy than if we had connected it to the M-template. It is possible that using the flow lines joining the two templates to let the templates “share” the 8”, sending some flow from M and some from L will be more efficient. This is not something that has been pursued further, however. Data for the Excel simulation for Scenario 2B, template L, is included in the appendix() if further details are required.

The criterion used was to stop production if the total flow went below 5 MSm³/day. This is because flows through a 14” pipe lower than 2.5 MSm³/day gives problems with liquid accumulation⁹. Simulating our model to its end, we find that the compression plateau lasts until August 2018, and the 5 MSm³/day-limit is reached at the start of 2026. This is summarized in the table below.

Table 6 Results of the end of natural plateau, total plateau and production for the flow optimization.

End of:	Year
Natural plateau	February 2017
Plateau	September 2019
Production	January 2026

⁹ Statoil/FRAMO presentation in Bergen

Stopping the production when reaching 5 MSm³/day is of course a major restriction in our model, but we have later gotten indications that Statoil's own simulation has been run several years longer. According to our findings, this is impossible with the lower flow limit we have been using. Therefore there has to be a way to avoid the problem of flow aggregation. One idea we have to achieve this is to utilize that installing the compressor also means that you will have a manifold before the towhead, as illustrated in the compressor sketch in part A. Therefore, it is possible to shut down one of the 14" and send the flow just through the 8" and the remaining 14", increasing the flow rate through these pipe. You will lose more pressure energy this way, but you can keep on producing longer. If this for some reason does not work, and if it is economically viable, there is plenty of time to develop new technology to deal with the aggregation problem before 2026.

As a final way to test our optimized production strategy, we've compared it with the default production strategy in a 'zero-case': a scenario without compressor, LPM, and just using the two 14" (together with the usual lower production limit). The optimized strategy had a recovery factor 0.76% higher than the default strategy, with production in both cases stopping in January 2022.

We think it is interesting that playing with production rates and the 8" can extend the plateau by over half a year. Of course everything depends on the correctness of our model; especially the equation for the reservoir pressure. As a final observation, note that shutting down the pipe from the M-template in 2009-2011 frees this pipe up for other uses. This brings us over to Scenario 2, which is directly linked to this.

4. Economical calculations

The economic analysis includes the evaluation of the economic value of compression in three different scenarios and the economic value of production management in 6 different cases.

4.1 General economy

In order to evaluate the economic value of each of the different scenarios and to evaluate the economic value of the compressor in our project an economic analysis was made with the following assumptions:

- Fixed 2013 Costs and oil/gas prices
- 1 USD = 6 NOK
- Oil Price: 100 USD13/barrel
- Gas Price: 2,30 NOK13/Sm³
- Net Present Value estimated at 8% discount factor.
- Taxation of net cash flow: 78%
- No depreciation

All the assumptions were provided by Statoil. For the Capital Expenditures (CAPEX) the following expenditures were taken into account:

- Framo Engineering \$156,380,316 USD for engineering, procurement and subsea compressor construction.
- Nexans \$100,778,426 USD for 16.5 km of subsea power umbilical.
- Subsea7 \$70,000,000 USD for engineering, installation and commissioning of a 10 mile integrated power service umbilical, a protection structure, a subsea compressor station, pipeline spools and tie-ins.
- 1,000 MNOK for Low Pressure Modification.
- The cost distribution for the Compressor CAPEX is 20% in year n-2, 40 % in year n-1 and 40 % in year n, where n is year the compressor started.

For the Operational Expenditures (OPEX) the analysis includes the following:

- Operational Cost per year for Energy, CO₂ and NO_x provided by Statoil.
- Sorco Contract for upgrading and replacement of control system, instrumentation and cables.
- Electricity for compressor considering assuming an average power consumption of 7.5 MW, and the price of kWh being 0,50 NOK.

For water production we assumed and water gas ratio (WGR) of 15 m³/million Sm³ in 2009 and increasing 0.25 m³/million Sm³ per year.

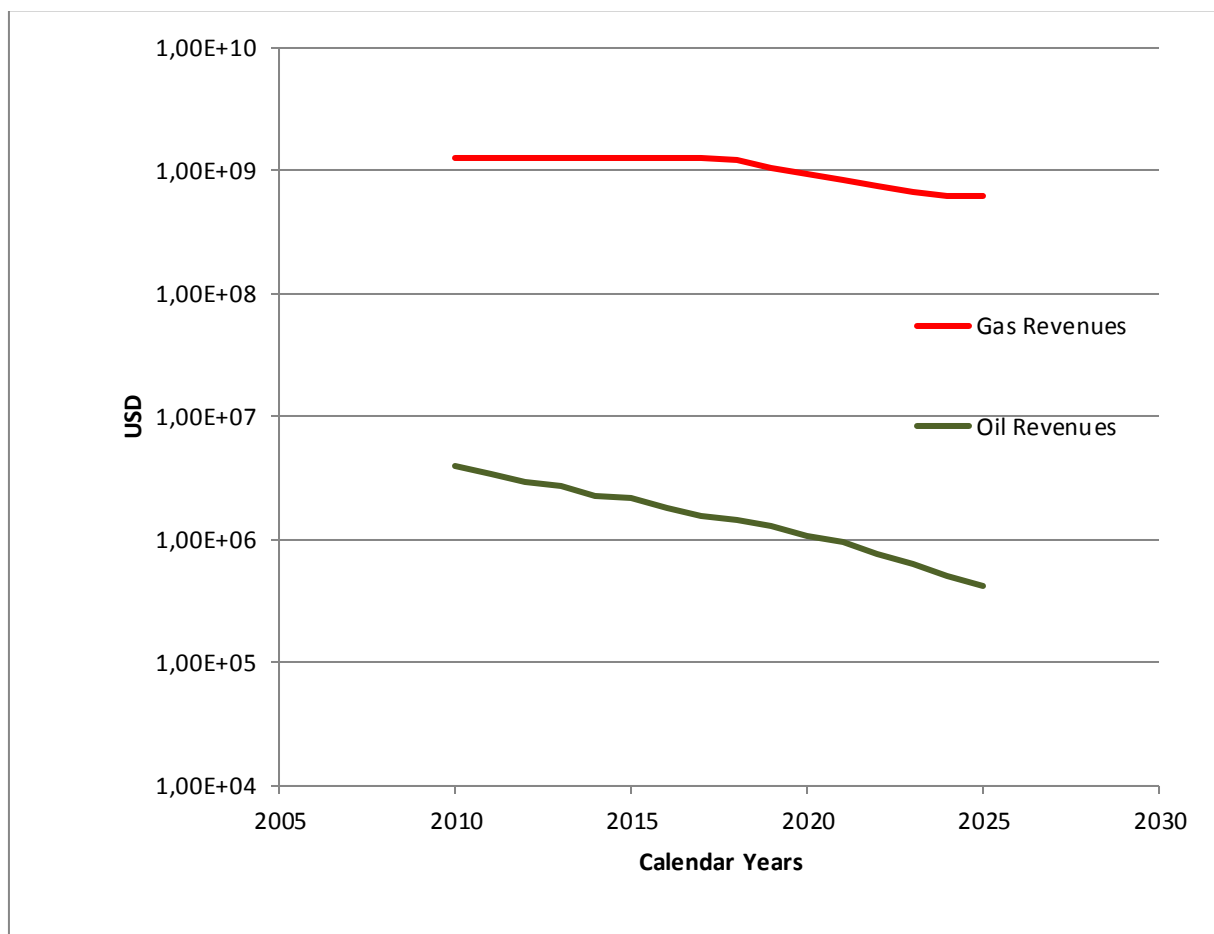


Figure 22: Comparison of revenues from oil and gas

Seeing as the revenues from oil are so small compared to the revenues from gas, the oil is simply ignored in our calculations.

4.2 Evaluating the NPV of the compressor project in different scenarios

As previously stated, the aim of the economic analysis is to evaluate the value added by the subsea compressor in three scenarios, which we summarize here:

- Scenario A: Do not use LPM, use two 14" pipes, default production strategy
- Scenario 1B: Use LPM, two 14" pipes and one 8" pipe, default production strategy
- Scenario 2B: Use LPM, from 2015 use one 14" pipe and one 8" pipe, optimized production strategy

The analysis in each of these scenarios is based on simulating two cases: one with compression and one without, keeping other variables fixed. To find out what value the compression project has in the different scenarios, revenues coming from the extra gas produced was used and then compared with the CAPEX and OPEX for the project, discounted and taxed as above.

In the part A case without compression, there is no compressor nor LPM, and so the production period ends already in 2022. The extra three years added by the compressor are extremely valuable, as is shown in the dramatic increase of NPV during the last three years. Also, even when using the default production strategy, and not utilizing the 8", one is able to keep the production running to 2025. The compression project is extremely valuable in this scenario. Compare with figure 23.

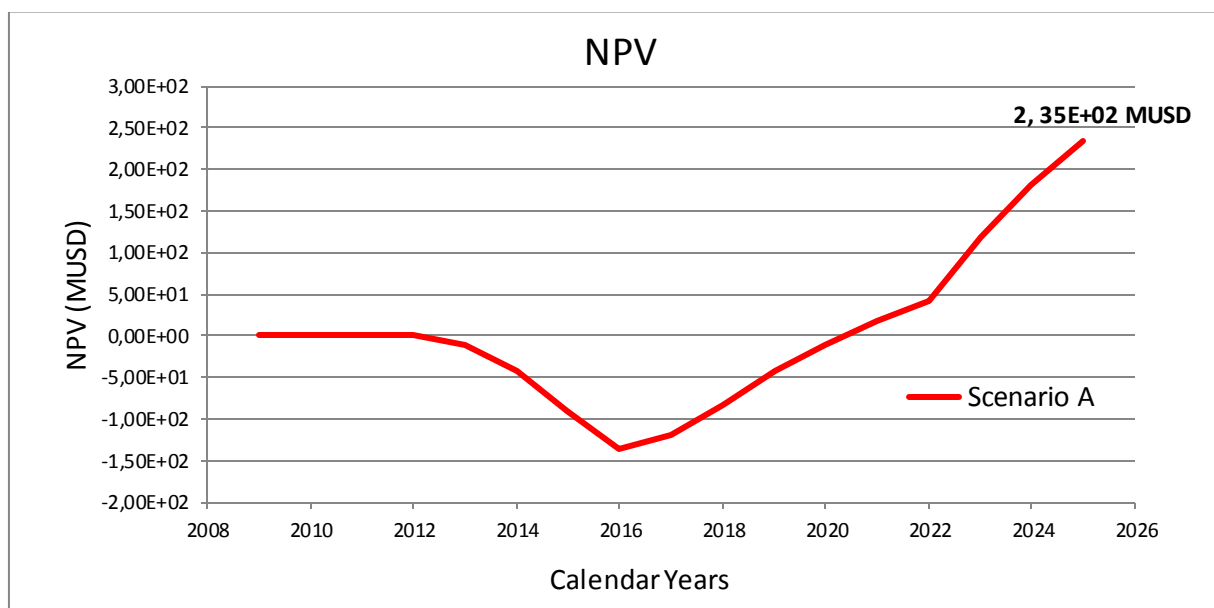


Figure 23: NPV for the Scenario A which evaluates the value of the compressor with no LP modification.

Table 7 shows the Break Even and the Internal Rate of Return for Scenario A.

Table 7: Break even and internal rate of return (IRR), scenario A

Scenario	Break Even	IRR
A, compression	2020	26,30 %

From figure 24 we see that in Scenario 1B we don't have positive NPV. If we in the calculations depreciate the CAPEX of the compressor, for example by writing off one sixth of its value over the first six years of compression, we'll get a positive NPV. This is because the CAPEX for the compressor is of the magnitude of 500 MUSD, and the tax benefits we get from depreciation will outweigh the 5 MUSD we're losing in the project, giving us positive NPV. However, as we see it, this doesn't justify the project. The economic loss just is just moved over to the government giving us the tax benefits. The extra year of production added by the compressor however, is what makes us more or less break even.

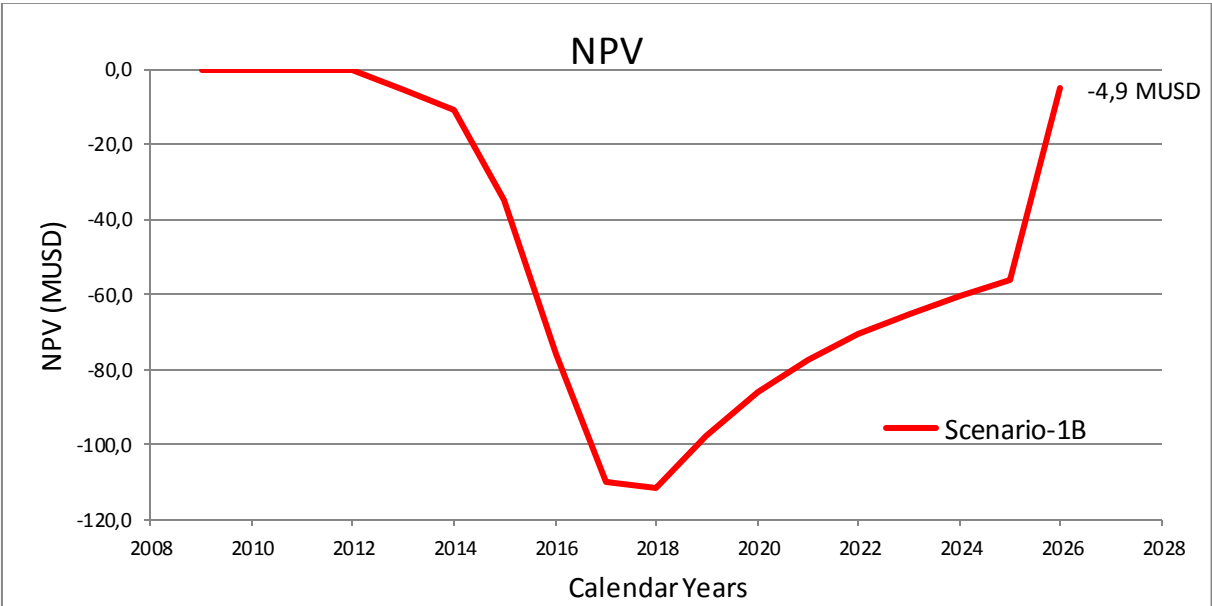


Figure 24: NPV for the Scenario 1B which evaluates the value of the compressor when shutting down a pipeline, with LPM.

Let's consider figure 25, showing that the NPV of the compression project is positive in Scenario 2B. This shows that not only does the flow optimization extend the plateau and increase the value of the production as a whole, but when comparing the effect of the compressor under this strategy, it is a strategy that seems to increase the value of the compressor project as well. This is because it is the additional years of production you get from the compressor that are really valuable, not so much the extra Sm3 of gas you're able to get in the years the field would have been producing anyway.

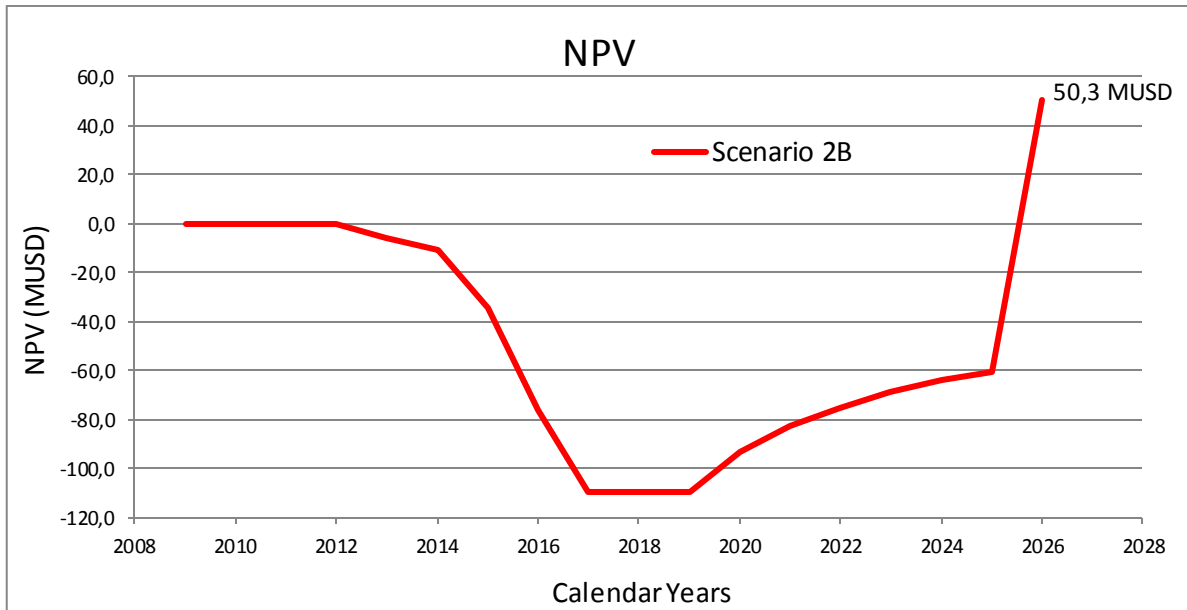


Figure 25: NPV for the Scenario 2B which evaluates the value of the compressor with flow optimization.

To sum up, the compression project seems to gravitate around an NPV of 0 if we use LPM and respect the 5 Msm³/day lower flow limit, and doesn't seem to be a robust investment under these restrictions. We need to continue for additional years for the compression to be valuable.

4.2 Evaluating the production management scenarios.

In this section the total NPVs for all six cases are given. As pointed out earlier, this is interesting because one gets the NPV for the total project under different operating conditions, showing the effect of the differences in the cases compared to the scale of the entire project. In figure 26 the NPVs for the cases are plotted as a function of time.

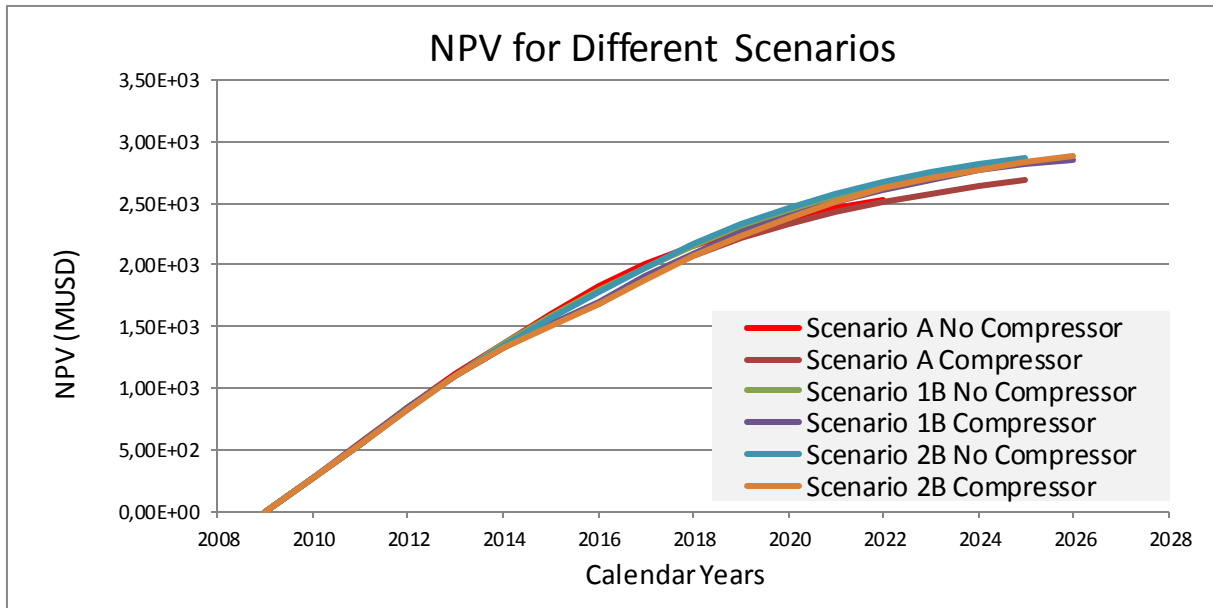


Figure 26: NPV plot showing the economic effect of producing in 6 different cases.

The effects of no expenditures related to the compressor and LPM are seen in the early years for Scenario A without compression, giving it the best NPV in the early years. After the natural plateau has ended the scenarios with the value-enhancing technology begin to dominate.

Table 8: NPV and Recovery Factors for different scenarios.

<i>Scenarios</i>	<i>NPV (Billion USD)</i>	<i>Recovery Factor</i>
A, no compression	2.53	0.508
A, compression	2.69	0.634
1B, no compression	2.85	0.633
1B, compression	2.86	0.677
2B, no compression	2.87	0.651
2B, compression	2.89	0.687

Table 8 really summarizes everything. This table also indicates the benefits of LPM, which adds a lot of value to the project. Note that the value added to the project by the compressor is much higher if

LPM isn't used. Much of the benefits related to compression seem to drown in the value added by the LPM.

Also, we see that the NPVs for the two cases within the same scenario are ordered in the correct way according to the results from section 4.2.

5. Summary and recommendations

All in all, it seems that that our simple model was a good approximation to reality. The results we have achieved seems reasonable and coherent.

Related to the performance of the compressor, a complete wet gas model would have been of great value in this project. With this, more realistic simulations could have been done to evaluate the performance of the compressor.

We have explored the NPV of the compression project under three different scenarios; in one of these we have optimized the production strategy, and we have seen that it outperforms our so-called 'default'-strategy. The 5 MSm³/day lower production limit we have used entails that the project will end in 2025-2026. Our economic analysis indicates that the project is not economically robust, but it seems that a lower flow limit will make the NPV positive. The critical factor is really how long the project has been run. If it's only run until the 5 MSm³/day limit, our conclusion is that the project is not economically feasible.

List of Symbols, abbreviation and Quantities used

CAPEX	Capital expenditure
Ct	Tubing coefficient 7" (ID=6.094")
DPchoke	Pressure difference over the choke
Error suction	Difference between pressures when mixing flows at the compressor intake (in reality 0)
Error ΔP_2	Difference in ΔP fixed compressor and ΔP
GIIP	Gas initially in place
GP	Gas produced
ΔGP	Change in gas produced
GP/G(GIIP)	Recovery factor
h	Hour
kW	Kilowatt
LPM	Low-pressure modification
m	Meter
N	Compressor speed (rpm)
OPEX	Operation expenditure
Plateau	Period with total production 10 M sm ³ /day
Pi	Initial reservoir pressure
Pr	Reservoir pressure
Psep	Separator pressure on platform
Ptowhead	Towhead pressure
Ptemplate	Template pressure
Psuck	Suction pressure compressor
Psuck average	Average suction pressure compressor
$\Delta P_{\text{compressor}}$	Pressure change over the compressor
ΔP	change in pressure
ΔP_{fixed}	Fixed change in pressure over the compressor
qf	Flow rate from template L or M
qw	Flow rate from well
qTot	The total flow rate from template L and M
Rs	Solution Gas oil Ratio
Sm ³ /day	Standard cubic meters per day
ΔT	Temperature change
Z	Compressibility factor
Td	Discharge temperature
TR	Temperature reservoir
°C	Degree centigrade

Literature

1. Statoil,
URL:<http://www.statoil.com/no/ouoperations/explorationprod/ncs/gullfaks/pages/default.aspx>, Published 2007-09-26, 14:13 CET. Updated 2013-04-09, 08:19 CET. 26/4-2013
2. Statoil,URL:<http://www.statoil.com/no/OurOperations/ExplorationProd/ncs/Gullfaks/Pages/GullfaksSouth.aspx>, 10/4-2013
3. Powerpoint presentation given by Anne Margrete Solheim in Bergen 20.02.2013, Statoil
4. Statoil,URL:http://www.statoil.com/no/NewsAndMedia/PressRoom/Downloads/gullfaks_field_layout.jpg. 26/4-2013.
5. Offshore, A. Gilja, 6/5-2009,
URL:http://www.offshore.no/sak/24835_lovende_subsea_teknologikontrakt_til_framo 26/4-2013
6. Offshore, J. Økland, 22/5-2012,
URL:http://www.offshore.no/sak/35196_tre_milliarder_girer_om_gullfaks_soer 26/4-2013
7. M, Golan, Sketch of process layout, 2013
8. Curtis H. Whitson and Michael R. Brule, 2000
9. S.C. Amundsen, “*Wet Gas Compression*”, NTNU, Master Thesis, 2009
10. Gudmundsson, JS. Kompresjon og Kompressorer, 2010
11. Boosting heating of subsea pipelines, 2003

List of appendix

Appendix 1	Relevant data from L and M template
Appendix 2	Excel sheet Part A
Appendix 3	Compressor map Part A
Appendix 4	Reservoir composition from Statoil
Appendix 5	HYSYS arrangement to generate black oil properties
Appendix 6	Results from comparison of dry gas model in excel and wet gas model in HYSYS, Parallel
Appendix 7	Results from comparison of dry gas model in excel and wet gas model in HYSYS, Series
Appendix 8	Results from sensitivity analyses regarding hydrate formation temperature
Appendix 9	Flow optimization Scenario 2B with compression, L-template

Appendix 1 Relevant data for template L and M given from Statoil

Gulfaks South L-M satellite system Pre-compression Phase (Start Jan 2009)	East Tank L-Template Fault Block 13 Brent Formation	West Tank M-Template Fault Block 14 Brent Formation	
G=GIIP-Gas cap (31 December 2008)		17,5E+9	Sm ³
Condnsate from Gas Cap (31 December 2008)		4,4E+6	Sm ³
oil legs: STOIP (31 December 2008)		7,5E+6	Sm ³
Gas in Solution (from oil leg)		1,9E+9	Sm ³
Rs Solution Gas oil Ratio (oil leg) (31 December 2008)		248	Sm ³ /Sm ³
rs Condensate gas ratio (gas cap) (31 December 2008)		251	Sm ³ /MSm ³
STOIP + Condensate (31 December 2008)	34,5E+6		Sm ³
GIIP + dissociative gas (31 December 2008)	54,2E+9		Sm ³
Daily Plateau production rate (per template)- Pre-compression mode	6,0E+6	4,0E+6	Sm ³ /d
Wells per template (Pre compression)	4	3	
Production days per year	328	330	day
T _R , Temperature reservoir	128	112	°C
P _i , initial Res pressure (01 Jan 2009)	240	210	bara
P _i , initial Res pressure (1999)	459	446	
C, inflow Back pressure coefficient	1000	700	Sm ³ /bar ²ⁿ
n, backpressure, exponent	0,8	0,8	
Tubing MD	3515	2800	
Tubing TVD	3100	2500	
C _t , Tubing coefficient 7" (ID=6.094")	38152,4	41163	Sm ³ /bar
Elevation coefficient Tubing, S	0,43	0,34	
C _{FL} 12".Template L-to-Towhead 66 m (ID=) Pre-compression spool	1403054		Sm ³ /bar
C _{FL} 8" Template-to-Towhead 62 m (Id=)	466786		Sm ³ /bar
C _{FL} 12".Template M-to-Towhead 64 m (ID=) compression spool		1397663	Sm ³ /bar
C _{PL Pipeline} 14" Towhead-to-GFC 14000m (ID=0.32m)	148220	148220	Sm ³ /bar
C _{PL Pipeline} 8" Towhead-to-GFC 14000m (N-Line) (ID=0.197m)	32967	32967	Sm ³ /bar
Separator pressure GFC (Inlet Sep)	60	60	bara
Tope GFC riser pressure (High pressure mode)	65	65	
Tope GFC riser pressure (Low pressure mode)	25	25	
Gas molecular weight (Methane)	19	19	kg/kmole
Gas specific gravity	0,66	0,66	Gas specific gravity

Appendix 2 Excel sheet Part A

Table 3 Data and results from template L

East tank, template L, 4 Wells																
Year cont	Δtime	Calendar year	qf (Sm ³ /day)	Δ Gp	Gp (Sm ³)	Gp/G	PR (bara)	Z	qw (Sm ³ /d)	Pwf (bara)	Pwh (bara)	Psep 2x14" (bara)	Ptowhead (bara)	Ptemp 12" (bara)	DpChoke (bar)	q tot field (Sm ³ /day)
0	0	2009	6,0E+6	0,00	0,00	0,00	240	0,957	1,5E+6	220	173	65	73	73,4	99,8	10,0E+6
1	1	2010	6,0E+6	2,0E+9	1,97E+09	0,04	231	0,953	1,5E+6	210	165	65	73	73,4	91,9	10,0E+6
2	1	2011	6,0E+6	2,0E+9	3,94E+09	0,07	222	0,948	1,5E+6	199	156	65	73	73,4	83,0	10,0E+6
3	1	2012	6,0E+6	2,0E+9	5,90E+09	0,11	212	0,945	1,5E+6	189	147	65	73	73,4	74,0	10,0E+6
4	1	2013	6,9E+6	2,3E+9	8,17E+09	0,15	201	0,941	1,7E+6	171	131	65	73	73,4	57,6	10,0E+6
5	1	2014	7,5E+6	2,5E+9	1,06E+10	0,20	190	0,938	1,9E+6	154	114	65	73	73,4	40,8	10,0E+6
6	1	2015	7,5E+6	2,5E+9	1,31E+10	0,24	178	0,936	1,9E+6	140	102	65	73	73,4	28,3	10,0E+6
7	1	2016	8,0E+6	2,6E+9	1,57E+10	0,29	167	0,934	2,0E+6	120	82	65	73	73,5	8,2	10,0E+6
7,5	0,5	2016,5	8,0E+6	1,3E+9	1,70E+10	0,31	161	0,934	2,0E+6	112	73	65	73	73,5	0,0	10,0E+6
8	0,5	2017	7,8E+6	1,3E+9	1,83E+10	0,34	155	0,934	1,9E+6	105	68	65	73	73,4	-5,2	10,0E+6
9	1	2018	7,6E+6	2,5E+9	2,08E+10	0,38	144	0,934	1,9E+6	90	53	65	73	73,4	-20,2	10,0E+6
9,645	0,645	2018,645	7,6E+6	1,6E+9	2,24E+10	0,41	137	0,934	1,9E+6	80	42	65	73	73,4	-31,7	10,0E+6
10	0,355	2019	7,3E+6	846,6E+6	2,33E+10	0,43	134	0,935	1,8E+6	78	41	65	73	72,8	-31,9	9,6E+6
11	1	2020	6,5E+6	2,1E+9	2,54E+10	0,47	125	0,936	1,6E+6	72	39	65	71	71,2	-31,9	8,5E+6
12	1	2021	5,9E+6	1,9E+9	2,73E+10	0,50	116	0,938	1,5E+6	67	38	65	70	70,0	-31,9	7,6E+6
13	1	2022	5,3E+6	1,7E+9	2,91E+10	0,54	109	0,940	1,3E+6	63	37	65	69	69,0	-31,9	6,8E+6
14	1	2023	4,8E+6	1,6E+9	3,06E+10	0,56	103	0,941	1,2E+6	59	36	65	68	68,2	-31,9	6,1E+6
15	1	2024	4,3E+6	1,4E+9	3,20E+10	0,59	97	0,943	1,1E+6	56	36	65	68	67,6	-31,9	5,4E+6
16	1	2025	3,9E+6	1,3E+9	3,33E+10	0,61	91	0,945	972,9E+3	54	35	65	67	67,1	-31,9	4,9E+6

Table 4 Results from template M

West tank, template M, 3 Wells																
Year cont	Δtime	Calendar year	qf (Sm ³ /day)	Δ Gp	Gp (Sm ³)	Gp/G	PR (bara)	Z	qw (sm ³ /d)	Pwf (bara)	Pwh (bara)	Psep 2x14" (bara)	Ptowhead (bara)	Ptemp 12" (bara)	DpChoke (bar)	q tot field (Sm ³ /day)
0	0	2009	4,0E+6	0,0E+00	0	0,00	210	0,926	1,3E+6	178	146	65	73	73,3	72,7	10,0E+6
1	1	2010	4,0E+6	1,3E+09	1,3E+9	0,08	194	0,921	1,3E+6	158	129	65	73	73,3	56,2	10,0E+6
2	1	2011	4,0E+6	1,3E+09	2,6E+9	0,15	177	0,918	1,3E+6	137	111	65	73	73,3	37,8	10,0E+6
3	1	2012	4,0E+6	1,3E+09	4,0E+9	0,23	161	0,917	1,3E+6	116	92	65	73	73,3	18,5	10,0E+6
4	1	2013	3,1E+6	1,0E+09	5,0E+9	0,28	149	0,917	1,0E+6	114	93	65	73	73,3	19,2	10,0E+6
5	1	2014	2,5E+6	8,3E+08	5,8E+9	0,33	139	0,918	8,3E+05	111	91	65	73	73,3	18,0	10,0E+6
6	1	2015	2,5E+6	8,3E+08	6,6E+9	0,38	129	0,920	8,3E+05	99	81	65	73	73,3	7,3	10,0E+6
7	1	2016	2,0E+6	6,6E+08	7,3E+9	0,42	122	0,922	6,7E+05	98	81	65	73	73,2	7,3	10,0E+6
7,5	0,5	2016,5	2,0E+6	3,3E+08	7,6E+9	0,44	118	0,923	6,7E+05	93	77	65	73	73,2	3,3	10,0E+6
8	0,5	2017	2,2E+6	3,6E+08	8,0E+9	0,46	114	0,924	7,3E+05	83	68	65	73	73,2	-5,2	10,0E+6
9	1	2018	2,4E+6	7,8E+08	8,8E+9	0,50	105	0,928	7,8E+05	67	53	65	73	73,3	-20,3	10,0E+6
9,645	0,645	2018,645	2,4E+6	5,2E+08	9,3E+9	0,53	99	0,930	8,1E+05	54	41	65	73	73,3	-31,9	10,0E+6
10	0,355	2019	2,3E+6	2,7E+08	9,6E+9	0,55	96	0,931	7,7E+05	53	41	65	73	72,6	-32,0	9,6E+6
11	1	2020	2,0E+6	6,5E+08	10,2E+9	0,58	88	0,935	6,6E+05	50	39	65	71	71,1	-32,0	8,5E+6
12	1	2021	1,7E+6	5,6E+08	10,8E+9	0,62	81	0,938	5,7E+05	48	38	65	70	69,9	-32,0	7,6E+6
13	1	2022	1,5E+6	4,9E+08	11,3E+9	0,64	76	0,941	4,9E+05	46	37	65	69	68,9	-32,0	6,8E+6
14	1	2023	1,3E+6	4,2E+08	11,7E+9	0,67	71	0,944	4,3E+05	45	36	65	68	68,1	-32,0	6,1E+6
15	1	2024	1,1E+6	3,7E+08	12,1E+9	0,69	67	0,947	3,7E+05	44	36	65	68	67,5	-32,0	5,4E+6
16	1	2025	969,7E+3	3,2E+08	12,4E+9	0,71	63	0,949	3,2E+05	43	35	65	67	67,0	-32,0	4,9E+6

Table 5 Results using solver in excel

Compressor									
Calendar year	P suck L (bara)	P suck M (bara)	P suck ave (bara)	Error suction	ΔP Compressor	rp comp	ΔP comp fix	Error ΔP ²	q tot field (Sm ³ /day)
2016,5									10,0E+6
2017	68,0	68,0	68,0	2,39E-15	5,2	1,1			10,0E+6
2018	52,9	52,9	52,9	2,13E-14	20	1,4			10,0E+6
2018,65	41,3	41,3	41,3	8,51E-14	32	1,8			10,0E+6
2019	40,6	40,6	40,6	1,28E-06	32	1,8	32	1,99E-11	9,6E+6
2020	39,0	39,1	39,0	1,04E-04	32	1,8	32	1,05E-10	8,5E+6
2021	37,8	37,85	37,8	3,84E-05	32	1,8	32	3,97E-11	7,6E+6
2022	36,9	36,9	36,9	4,47E-05	32	1,9	32	3,34E-11	6,8E+6
2023	36,1	36,1	36,1	2,79E-07	32	1,9	32	4,76E-12	6,1E+6
2024	35,5	35,5	35,5	1,14E-05	32	1,9	32	5,89E-12	5,4E+6
2025	35,0	35,0	35,0	4,86E-12	32	1,9	32	4,66E-05	4,9E+6

Appendix 3

Compressor map Part A

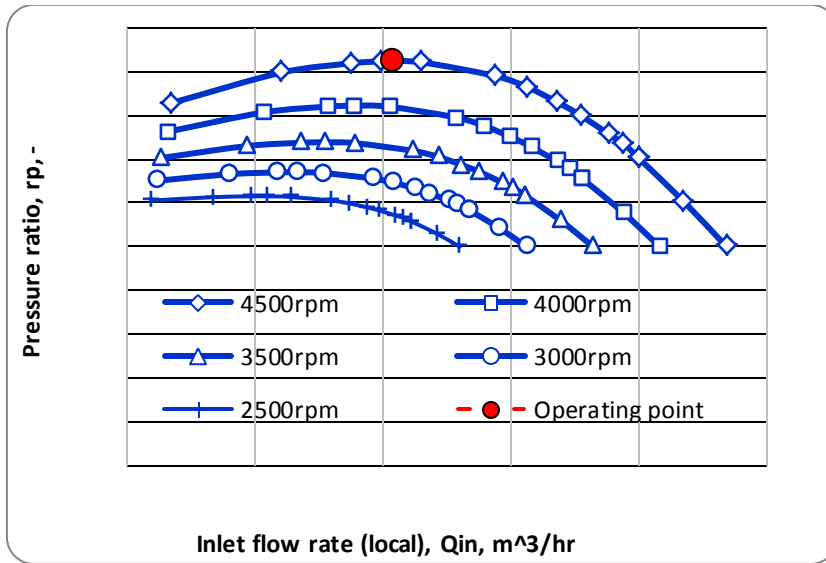


Figure 9: Compressor in parallel 2021. Inlet flow vs pressure ratio

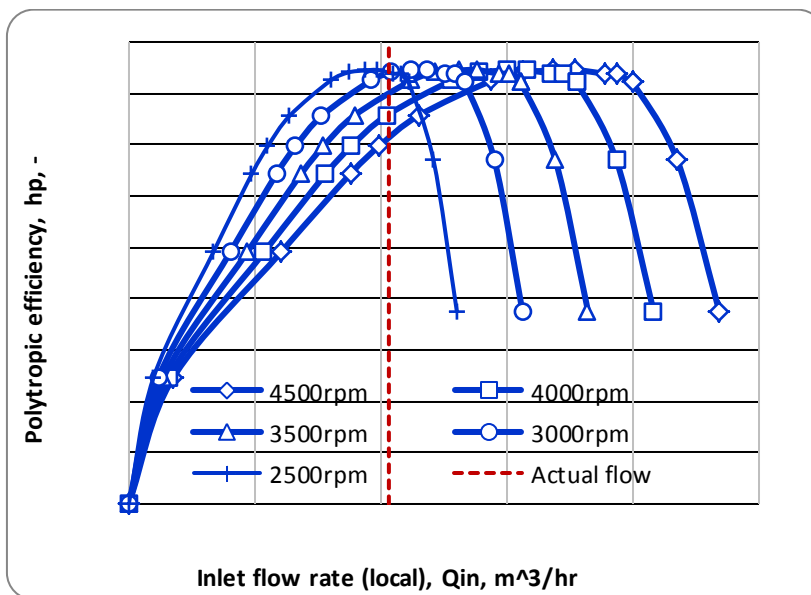


Figure 10: Compressor in parallel 2021. Inlet flow vs polytropic efficiency

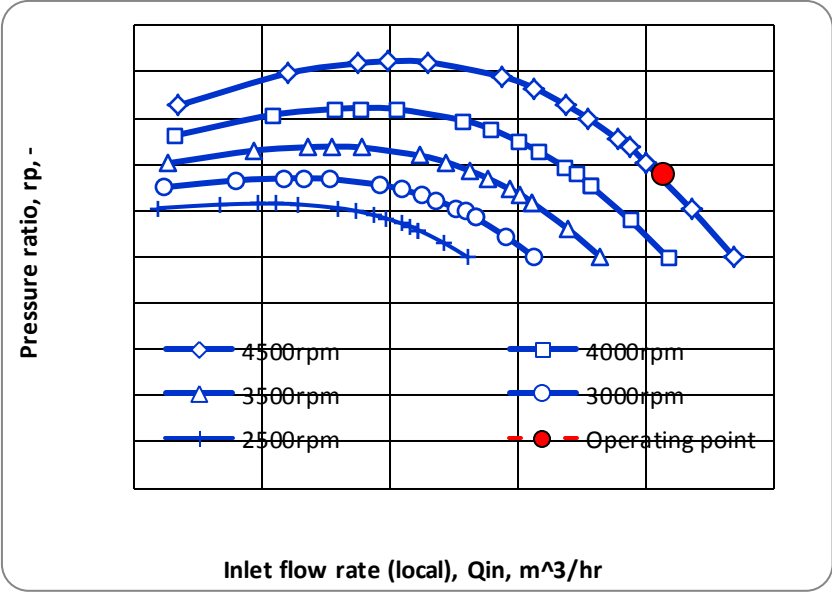


Figure 11: Compressor in series 2021. Inlet flow vs pressure ratio

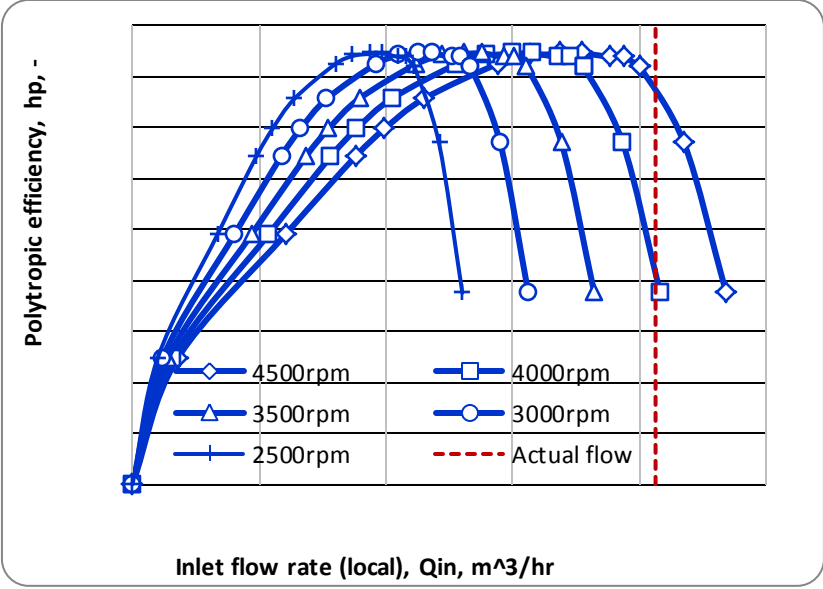


Figure 12: : Compressor in series 2021. Inlet flow vs polytropic efficiency

Appendix 4:

Reservoir composition from Statoil

Component	mole%
Nitrogen	0,24
CO ₂	1,56
Methane	86,1
Ethane	5,55
Propane	2,1
i-Butane	0,29
n-Butane	0,64
i-pentane	0,2
n-pentane	0,26
n-hexane	0,32
Cyclopentane	0,08
Benzene	0,12
Cyclohexane	0,14
n-heptane	0,23
Methylcyclohexane	0,19
Toluene	0,2
n-octane	0,24
E-Benzene	0,02
M-Xylene	0,1
O-Xylene	0,03
n-nonane	0,18
C ₁₀₊	1,21
SUM:	100
Properties of C ₁₀₊	
C ₁₀₊ molv.(g/mol)	200
Ideal liquid density [kg/m ³]	814

Appendix 4: Calculation method for material balance

“The basis of calculation is 1bbl reservoir bulk volume. The conservation-of-mass equations for single-cell material balance yields the following difference equations for reservoir-oil and –gas phases during the time step $\Delta t_k = t_k - t_{k-1}$ with a change in average pressure from $(\bar{P}_R)_{k-1}$ to $(\bar{P}_R)_k$.” (Curtis H. Whitson and Michael R. Brule, 2000)

In our calculations 1 year is taken as a time step.

$$(A_o)_k - (A_o)_{k-1} + \Delta N_p = 0 \quad \text{and} \quad (A_g)_k - (A_g)_{k-1} + \Delta G_p = 0 \quad ,$$

where ΔN_p and ΔG_p = incremental quantities of total surface oil and total surface gas, respectively, produced during the timestep;

$$A_o = \emptyset \left[\frac{S_o}{B_o} + \frac{5.615(1 - S_w - S_o)r_s \gamma_o^*}{B_{gd}} \right]$$

and

$$A_g = \emptyset \left[\frac{S_o R_s \gamma_g^*}{B_o} + \frac{5.615(1 - S_w - S_o)}{B_{gd}} \right]$$

$$\gamma_o^* = \frac{\gamma_{og}}{\gamma_{oo}}$$

$$\gamma_g^* = \frac{\gamma_{og}}{\gamma_{oo}}$$

ΔN_p and A_o are in STB/bbl, ΔG_p and A_g are in scf/bbl, ΔG_p and A_g are in scf/bbl, R_s is in scf/STB, r_s is in STB/scf, and B_{gd} is in ft³/scf. Other quantities used in the material-balance procedure are

$$E_o = 1 + 5.615 r_s \gamma_o^* \frac{k_{rg} \mu_o B_o}{k_{ro} \mu_g B_{gd}}$$

$$E_g = R_s \gamma_g^* + 5.615 r_s \frac{k_{rg} \mu_o B_o}{k_{ro} \mu_g B_{gd}}$$

$$R_p = \frac{\Delta G_p}{\Delta N_p}$$

$$\frac{k_{rg}}{k_{ro}} = f(S_o)$$

Application of these relations for gas-condensate reservoirs is shown step by step.

1. Specify $(\Delta G_p)_k$, total surface gas produced in scf/bbl of bulk volume.

2. Assume $(\bar{P}_R)_k$ and calculate PVT properties and porosity:

$(B_o)_k, (R_s)_k, (\mu_o)_k, (\gamma_o^*)_k, (B_{gd})_k, (r_s)_k, (\mu_g)_k, (\gamma_g^*)_k$ and $(\phi)_k$

3. Calculate oil saturation $(S_o)_k$:

$$(S_o)_k = \frac{(A_g)_{k-1} + (\Delta G_p)_k - [\phi(1 - S_w)/B_{gd}]}{\left[\phi \left(R_s \gamma_g^* / B_o - \frac{1}{B_{gd}} \right) \right]_k}$$

4. Calculate $(k_{rg}/k_{ro})_k$ from $(S_o)_k$.

5. Calculate $(A_o)_k, (A_g)_k, (E_o)_k$ and $(E_g)_k$.

6. Calculate ΔN_{po} , incremental surface oil produced from reservoir oil, where $\Delta N_{po} = \Delta G_p / \bar{E}_g$ and $\bar{E}_g = 0.5 [(E_g)_k + (E_g)_{k+1}]$

7. Calculate ΔN_p , incremental total surface oil produced, where $\Delta N_{po} = \Delta N_p / \bar{E}_o$ and $\bar{E}_o = 0.5 [(E_o)_k + (E_o)_{k+1}]$

8. Calculate the material balance error,

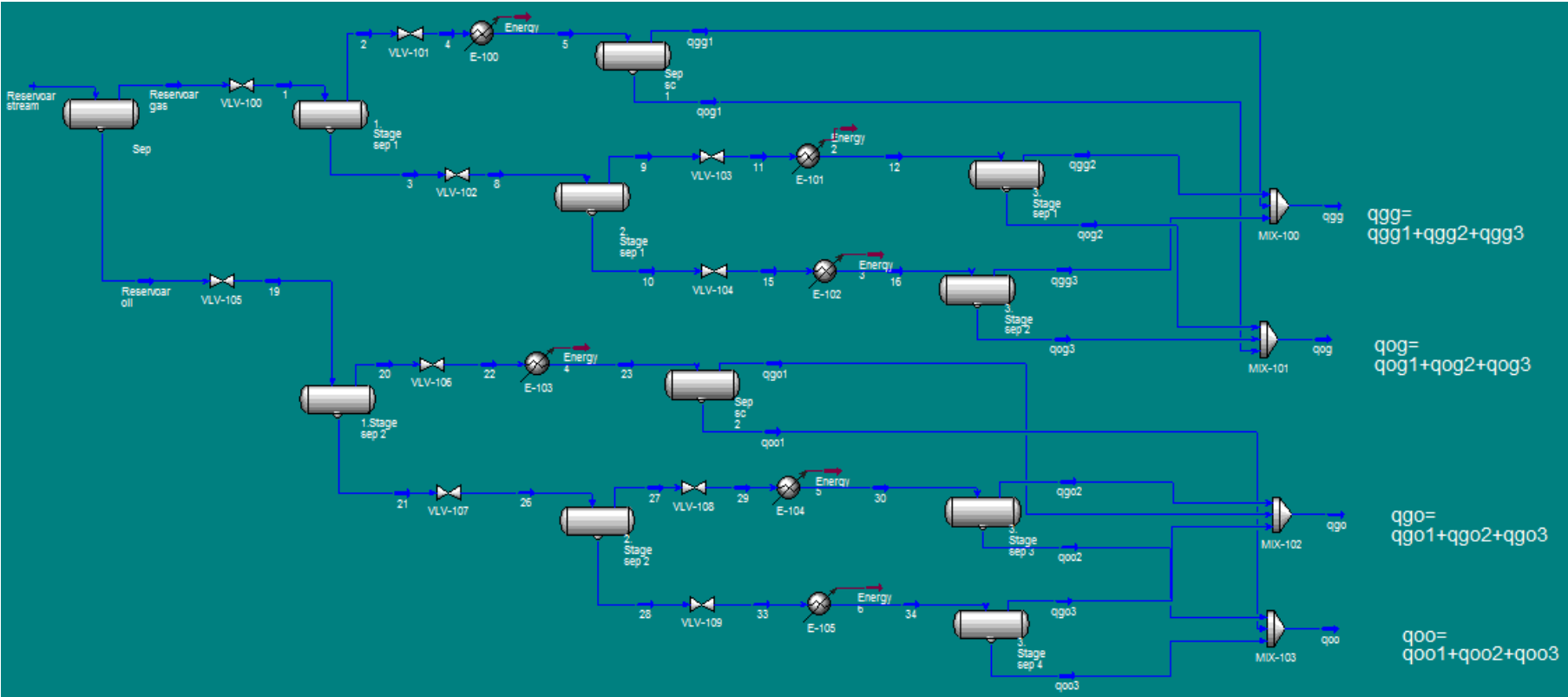
$$\varepsilon = (A_g)_k - (A_g)_{k-1} + \Delta G_p$$

If the error is not sufficiently assume a new pressure $(P_R)_k$

Above steps are followed by using IPT MATBAL programming software developed by Milan Stanko, PhD.

Appendix 5:

HYSYS arrangement to generate black oil properties



Appendix 6:

Results from comparison of dry gas model in excel and wet gas model in HYSYS, Parallel

2016

Flow[MSm ³ /d]	10
Suction Pressure[bara]	68
Discharge Pressure[bara]	73
Polytropic efficiency	0,62

	Excel	HYSYS	Difference	%
Outlet temperature of compressor [°C]	47,6	40,7	6,9	14,5
Power consumption[MW]	0,61	0,60	0,01	1,6
Actual inlet flow rate[m ³ /h]	2787,9	2737	50,9	1,8
Polytropic head[m]	853,4	694,6	158,8	18,6
Polytropic exponent[-]	2,3	1,42	0,9	38,3

2017

Flow[MSm ³ /d]	10
Suction Pressure[bara]	52,9
Discharge Pressure[bara]	73
Polytropic efficiency	0,84

	Excel	HYSYS	Difference	%
Outlet temperature of compressor [°C]	74,7	55,97	18,7	25,1
Power consumption[MW]	2,22	2,10	0,12	5,4
Actual inlet flow rate[m ³ /h]	3754,4	3634	120,4	3,2
Polytropic head[m]	4228,1	3328	900,1	21,3
Polytropic exponent[-]	1,6	1,26	0,3	21,3

2018

Flow[MSm ³ /d]	10
Suction Pressure[bara]	41,3
Discharge Pressure[bara]	73
Polytropic efficiency	0,81

	Excel	HYSYS	Difference	%
Outlet temperature of compressor [°C]	106,2	73,77	32,4	30,5
Power consumption[MW]	4,41	4,10	0,31	7,0
Actual inlet flow rate[m ³ /h]	4918,2	4782	136,2	2,8
Polytropic head[m]	7983,9	6208	1775,9	22,2
Polytropic exponent[-]	1,58	1,26	0,3	20,3

2019

Flow[MSm ³ /d]	9,6
Suction Pressure[bara]	40,6
Discharge Pressure[bara]	73
Polytropic efficiency	0,79

	Excel	HYSYS	Difference	%
Outlet temperature of compressor [°C]	110,7	75,73	35,0	31,6
Power consumption[MW]	4,5	4,17	0,33	7,3
Actual inlet flow rate[m ³ /h]	4802,9	4674,0	128,9	2,7
Polytropic head[m]	8273,32	6427	1846,3	22,3
Polytropic exponent[-]	1,60	1,27	0,3	20,6

2020

Flow[MSm ³ /d]	8,5
Suction Pressure[bara]	39
Discharge Pressure[bara]	71
Polytropic efficiency	0,75

	Excel	HYSYS	Difference	%
Outlet temperature of compressor [°C]	115,6	78,3	37,3	32,3
Power consumption[MW]	4,36	4,01	0,35	8,0
Actual inlet flow rate[m ³ /h]	4478,2	4322,0	156,2	3,5
Polytropic head[m]	8593,97	6619	1975,0	23,0
Polytropic exponent[-]	1,63	1,29	0,3	20,9

2021

Flow[MSm ³ /d]	7,6
Suction Pressure[bara]	37,8
Discharge Pressure[bara]	70
Polytropic efficiency	0,71

	Excel	HYSYS	Difference	%
Outlet temperature of compressor [°C]	121,7	82,7	39,0	32,0
Power consumption[MW]	4,27	4,02	0,25	5,9
Actual inlet flow rate[m ³ /h]	4129,3	4001,0	128,3	3,1
Polytropic head[m]	8911,2	7038	1873,2	21,0
Polytropic exponent[-]	1,67	1,31	0,4	21,6

2022

Flow[MSm ³ /d]	6,8
---------------------------	-----

Suction Pressure[bara] 36,9
 Discharge Pressure[bara] 69
 Polytropic efficiency 0,64

	Excel	HYSYS	Difference	%
Outlet temperature of compressor [°C]	134,3	86,56	47,7	35,5
Power consumption[MW]	4,38	4,01	0,37	8,4
Actual inlet flow rate[m ³ /h]	3784,7	3675,0	109,7	2,9
Polytropic head[m]	9196,5	7059	2137,5	23,2
Polytropic exponent[-]	1,81	1,36	0,5	24,9

2023

Flow[M³/d] 6,1
 Suction Pressure[bara] 36,1
 Discharge Pressure[bara] 68
 Polytropic efficiency 0,6

	Excel	HYSYS	Difference	%
Outlet temperature of compressor [°C]	143,4	90,15	53,3	37,1
Power consumption[MW]	4,29	3,91	0,38	8,9
Actual inlet flow rate[m ³ /h]	3470,4	3375,0	95,4	2,7
Polytropic head[m]	9412,5	7204	2208,5	23,5
Polytropic exponent[-]	1,91	1,39	0,5	27,2

2024

Flow[M³/d] 5,4
 Suction Pressure[bara] 35,5
 Discharge Pressure[bara] 68
 Polytropic efficiency 0,51

	Excel	HYSYS	Difference	%
Outlet temperature of compressor [°C]	170,4	100,5	69,9	41,0
Power consumption[MW]	4,74	4,27	0,47	9,9
Actual inlet flow rate[m ³ /h]	3124,1	3043,0	81,1	2,6
Polytropic head[m]	9980,76	7550	2430,8	24,4
Polytropic exponent[-]	2,27	1,50	0,8	33,9

2025

Flow[MSm ³ /d]	4,9
Suction Pressure[bara]	35
Discharge Pressure[bara]	67
Polytropic efficiency	0,51

	Excel	HYSYS	Difference	%
Outlet temperature of compressor [°C]	177,3	104,2	73,1	41,2
Power consumption[MW]	4,6	4,14	0,46	10,0
Actual inlet flow rate[m ³ /h]	2875,3	2804,0	71,3	2,5
Polytropic head[m]	10053,1	7603	2450,1	24,4
Polytropic exponent[-]	2,41	1,54	0,9	36,1

Appendix 7:

Results from comparison of dry gas model in excel and wet gas model in HYSYS, Series

2016

Flow[MSm ³ /d]	10
Suction Pressure[bara]	68
Discharge Pressure[bara]	73
Middle Pressure	70,46
Polytropic efficiency	0,55

	Excel	HYSYS	Difference	%
Outlet temperature of compressor [°C]	42,0	38,08	3,9	9,3
Power consumption[MW]	0,69	0,67	0,02	2,9
Actual inlet flow rate[m ³ /h]	5575,9	5473,0	102,9	1,8
Polytropic head[m]	422,95	346,3	76,7	18,1
Polytropic exponent[-]	2,76	1,50	1,3	45,7

2017

Flow[MSm ³ /d]	10
Suction Pressure[bara]	52,9
Discharge Pressure[bara]	73
Middle Pressure	62,14
Polytropic efficiency	0,5

	Excel	HYSYS	Difference	%
Outlet temperature of compressor [°C]	68,4	50,41	18,0	26,3
Power consumption[MW]	3,74	3,54	0,20	5,3
Actual inlet flow rate[m ³ /h]	7508,8	7267,7	241,1	3,2
Polytropic head[m]	2094,6	1656	438,6	20,9
Polytropic exponent[-]	2,77	1,54	1,2	44,4

2018

Flow[MSm ³ /d]	10
---------------------------	----

Suction Pressure[bara] 41,3
 Discharge Pressure[bara] 73
 Middle Pressure 54,91
 Polytropic efficiency 0,55

	Excel	HYSYS	Difference	%
Outlet temperature of compressor [°C]	86,0	60,72	25,3	29,4
Power consumption[MW]	6,31	6,00	0,31	4,9
Actual inlet flow rate[m ³ /h]	9836,4	9564,8	271,6	2,8
Polytropic head[m]	3880,8	3058,0	822,8	21,2
Polytropic exponent[-]	2,16	1,45	0,7	32,9

2019

Flow[M³m³/d] 9,6
 Suction Pressure[bara] 40,6
 Discharge Pressure[bara] 73
 Middle Pressure 54,44
 Polytropic efficiency 0,55

	Excel	HYSYS	Difference	%
Outlet temperature of compressor [°C]	87,7	61,52	26,2	29,9
Power consumption[MW]	6,26	5,90	0,36	5,8
Actual inlet flow rate[m ³ /h]	9605,7	9348,6	257,1	2,7
Polytropic head[m]	4006,7	3158,4	848,3	21,2
Polytropic exponent[-]	2,16	1,44	0,7	33,3

2020

Flow[M³m³/d] 8,5
 Suction Pressure[bara] 39
 Discharge Pressure[bara] 71
 Middle Pressure 52,62
 Polytropic efficiency 0,73

	Excel	HYSYS	Difference	%
Outlet temperature of compressor [°C]	74,1	56,53	17,6	23,7
Power consumption[MW]	4,23	3,98	0,25	5,9
Actual inlet flow rate[m ³ /h]	8952,4	8644,8	307,6	3,4
Polytropic head[m]	4054,3	3201,3	853,0	21,0
Polytropic exponent[-]	1,66	1,29	0,4	22,3

2021

Flow[M³m³/d] 7,6
 Suction Pressure[bara] 37,8
 Discharge Pressure[bara] 70
 Middle Pressure 51,44

Polytropic efficiency 0,79

	Excel	HYSYS	Difference	%
Outlet temperature of compressor [°C]	71,3	55,82	15,5	21,7
Power consumption[MW]	3,58	3,39	0,19	5,3
Actual inlet flow rate[m ³ /h]	8258,6	8001,9	256,7	3,1
Polytropic head[m]	4153,1	3295,8	857,3	20,6
Polytropic exponent[-]	1,57	1,26	0,3	19,7

2022

Flow[M³m³/d] 6,8
 Suction Pressure[bara] 36,9
 Discharge Pressure[bara] 69
 Middle Pressure 50,46
 Polytropic efficiency 0,80

	Excel	HYSYS	Difference	%
Outlet temperature of compressor [°C]	71,4	55,9	15,5	21,7
Power consumption[MW]	3,21	3,05	0,16	5,0
Actual inlet flow rate[m ³ /h]	7569,5	7350,8	218,7	2,9
Polytropic head[m]	4217,0	3355,2	861,8	20,4
Polytropic exponent[-]	1,56	1,26	0,3	19,2

2023

Flow[M³m³/d] 6,1
 Suction Pressure[bara] 36,1
 Discharge Pressure[bara] 68
 Middle Pressure 49,55
 Polytropic efficiency 0,84

	Excel	HYSYS	Difference	%
Outlet temperature of compressor [°C]	69,6	55,2	14,4	20,7
Power consumption[MW]	2,74	2,60	0,14	5,1
Actual inlet flow rate[m ³ /h]	6940,7	6750,0	190,7	2,7
Polytropic head[m]	4254,7	3395,7	859,0	20,2
Polytropic exponent[-]	1,51	1,24	0,3	17,9

2024

Flow[M³m³/d] 5,4
 Suction Pressure[bara] 35,5
 Discharge Pressure[bara] 68
 Middle Pressure 49,13
 Polytropic efficiency 0,85

	Excel	HYSYS	Difference	%
Outlet temperature of compressor [°C]	70,6	55,72	14,9	21,1

Power consumption[MW]	2,49	2,37	0,12	4,8
Actual inlet flow rate[m ³ /h]	6248,1	6085,2	162,9	2,6
Polytropic head[m]	4371,23	3492,0	879,2	20,1
Polytropic exponent[-]	1,51	1,24	0,3	17,9

2025

Flow[MSm ³ /d]	4,9
Suction Pressure[bara]	35
Discharge Pressure[bara]	67
Middle Pressure	48,43
Polytropic efficiency	0,85

	Excel	HYSYS	Difference	%
Outlet temperature of compressor [°C]	69,9	55,7	14,2	20,3
Power consumption[MW]	2,25	2,15	0,10	4,4
Actual inlet flow rate[m ³ /h]	5750,6	5607,7	142,9	2,5
Polytropic head[m]	4362,4	3494,3	868,1	19,9
Polytropic exponent[-]	1,49	1,24	0,3	16,8

Appendix 8:

Results from sensitivity analyses regarding hydrate formation temperature.

For the 14" pipeline

Overall Heat Transfer Coefficient [W/m²K] = 1,0

Molar Flow [kmol/h]	Flow Rate [MSm ³ /d]	Temperature of gas out of pipeline [°C]
4400	2,5	70,38
5300	3,0	71,99
6170	3,5	72,49
7050	4,0	72,05
7920	4,5	70,27
8810	5,0	65,09

Overall Heat Transfer Coefficient [W/m²K] = 2,0

Molar Flow [kmol/h]	Flow Rate [MSm ³ /d]	Temperature of gas out of pipeline [°C]
4400	2,5	57,58
5300	3,0	60,78
6170	3,5	62,54
7050	4,0	63,15
7920	4,5	62,37
8810	5,0	58,34

**Overall Heat Transfer Coefficient [W/m²K]
= 3,0**

Molar Flow [kmol/h]	Flow Rate [MSm ³ /d]	Temperature of gas out of pipeline [°C]
4400	2,5	47,25
5300	3,0	51,28
6170	3,5	53,92
7050	4,0	55,35
7920	4,5	55,34
8810	5,0	52,17

**Overall Heat Transfer Coefficient [W/m²K]
= 4,0**

Molar Flow [kmol/h]	Flow Rate [MSm ³ /d]	Temperature of gas out of pipeline [°C]
4400	2,5	39,28
5300	3,0	43,5
6170	3,5	46,57
7050	4,0	48,49

7920	4,5	49,03
8810	5,0	46,51

Overall Heat Transfer Coefficient [W/m²K]

= 5,0

Molar Flow [kmol/h]	Flow Rate [MSm ³ /d]	Temperature of gas out of pipeline [°C]
4400	2,5	32,69
5300	3,0	37,24
6170	3,5	40,31
7050	4,0	42,56
7920	4,5	43,46
8810	5,0	41,51

Overall Heat Transfer Coefficient [W/m²K]

= 6,0

Molar Flow [kmol/h]	Flow Rate [MSm ³ /d]	Temperature of gas out of pipeline [°C]
4400	2,5	27,29
5300	3,0	31,9
6170	3,5	35,19
7050	4,0	37,39
7920	4,5	38,52
8810	5,0	37,07

Overall Heat Transfer Coefficient [W/m²K]

= 7,0

Molar Flow [kmol/h]	Flow Rate [MSm ³ /d]	Temperature of gas out of pipeline [°C]
4400	2,5	22,89
5300	3,0	27,39
6170	3,5	30,74
7050	4,0	33,05
7920	4,5	34,16
8810	5,0	33,1

For the 8" pipeline

Overall Heat Transfer Coefficient [W/m²K] = 0,5

Molar Flow [kmol/h]	Flow Rate [MSm ³ /d]	Temperature of gas out of pipeline [°C]
700	0,4	61,39
1050	0,6	67,21
1400	0,8	69,43
1760	1,0	70,05
2105	1,2	69,38
2458	1,4	64,62

Overall Heat Transfer Coefficient [W/m²K] = 1,0

Molar Flow [kmol/h]	Flow Rate [MSm ³ /d]	Temperature of gas out of pipeline [°C]
700	0,4	44,59
1050	0,6	54,34
1400	0,8	59,22
1760	1,0	61,22
2105	1,2	61,08
2458	1,4	57,73

Overall Heat Transfer Coefficient [W/m²K] = 1,5

Molar Flow [kmol/h]	Flow Rate [MSm ³ /d]	Temperature of gas out of pipeline [°C]
700	0,4	32,28
1050	0,6	43,78
1400	0,8	50,31
1760	1,0	53,72
2105	1,2	54,47
2458	1,4	51,54

Overall Heat Transfer Coefficient [W/m²K] = 2,0

Molar Flow [kmol/h]	Flow Rate [MSm ³ /d]	Temperature of gas out of pipeline [°C]
700	0,4	23,72
1050	0,6	35,13
1400	0,8	42,66
1760	1,0	47,02
2105	1,2	48,64
2458	1,4	46,37

Appendix 9: Flow optimization Scenario 2B with compression, L-template

East tank, template L, 4 Wells																		
Year cont	Δ time	Calendar year	q_f (Sm ³ /day)	Δ G p (Sm ³)	Gp (Sm ³)	Gp/G	P_R (bara)	Z	q_w (Sm ³ /day)	P_{wf} (bara)	P_{wh} (bara)	$qf(8")$ (Sm ³ /day)	$qf(14")$ (Sm ³ /day)	$P_{towhead}$ (bara)	$P_{platform}$ (bara)	DP_{choke} (bar)	P_{sep} (bara)	q_{tot} (Sm ³ /day)
0,0	0	2009	6,0E+6	0,00E+00	0,00E+00	0,00	240,0	0,957	1,5E+06	220	173,17	000E+0	6,00E+06	173,1	168,3	103,3	65	10,0E+6
1,0	1	2010	10,0E+6	3,28E+09	3,28E+09	0,06	225,5	0,950	2,5E+06	182	131,80	1,8E+6	8,18E+06	131,7	119,6	54,6	65	10,0E+6
2,0	1	2011	10,0E+6	3,28E+09	6,56E+09	0,12	209,5	0,944	2,5E+06	162	113,22	1,8E+6	8,18E+06	113,1	98,7	33,7	65	10,0E+6
3,0	1	2012	10,0E+6	3,28E+09	9,84E+09	0,18	193,8	0,939	2,5E+06	141	93,19	1,8E+6	8,18E+06	93,0	74,9	9,9	65	10,0E+6
3,3	0,25	2012,25	10,0E+6	8,20E+08	1,07E+10	0,20	189,2	0,938	2,5E+06	135	86,89	1,8E+6	8,18E+06	86,7	66,9	1,9	65	10,0E+6
4,3	1	2013,25	7,5E+6	2,46E+09	1,31E+10	0,24	178,3	0,936	1,9E+06	140	101,49	1,4E+6	6,13E+06	101,4	92,6	27,6	65	10,0E+6
5,3	1	2014,25	7,5E+6	2,46E+09	1,56E+10	0,29	167,3	0,934	1,9E+06	125	88,33	1,4E+6	6,13E+06	88,2	77,9	12,9	65	10,0E+6
5,8	0,5	2014,75	7,5E+6	1,23E+09	1,68E+10	0,31	161,7	0,934	1,9E+06	117	81,27	1,4E+6	6,13E+06	81,2	69,8	4,8	65	10,0E+6
6,3	0,5	2015,25	7,2E+6	1,18E+09	1,80E+10	0,33	156,5	0,934	1,8E+06	113	78,22	1,3E+6	5,89E+06	78,1	67,3	2,3	65	10,0E+6
6,8	0,5	2015,75	6,8E+6	1,12E+09	1,91E+10	0,35	151,7	0,934	1,7E+06	110	76,87	1,2E+6	5,56E+06	76,8	67,0	2,0	65	10,0E+6
7,3	0,5	2016,25	6,4E+6	1,05E+09	2,02E+10	0,37	147,1	0,934	1,6E+06	107	75,96	1,2E+6	5,23E+06	75,9	67,1	2,1	65	10,0E+6
7,8	0,5	2016,75	6,0E+6	9,84E+08	2,11E+10	0,39	142,9	0,934	1,5E+06	105	75,44	1,1E+6	4,91E+06	75,4	67,7	2,7	65	10,0E+6
8,1	0,35	2017,1	5,80E+6	6,66E+08	2,18E+10	0,40	140,0	0,934	1,5E+06	103	74,29	1,1E+6	4,74E+06	74,2	67,0	2,0	65	10,0E+6
9,1	1	2018,1	6,32E+6	2071384783	2,39E+10	0,44	131,1	0,935	1,4E+06	93	65,48	2E+06	4,74E+06				65	10,0E+6
9,6	0,5	2018,6	6,19E+6	1015434313	2,49E+10	0,46	126,8	0,936	1,5E+06	80	50,21	2E+06	4,65E+06				65	10,0E+6
10,1	0,5	2019,10	6,30E+6	1033215875	2,59E+10	0,48	122,4	0,936	1,6E+06	71	40,11	2E+06	4,73E+06				65	10,0E+6
10,7	0,6	2019,7	6,41E+6	1261122120	2,72E+10	0,50	117,1	0,938	1,6E+06	60	23,89	2E+06	4,81E+06				29	10,0E+6
11	0,3	2020	6,33E+6	622648270	2,78E+10	0,51	114,5	0,938	1,6E+06	56	18,18	2E+06	4,75E+06				25	9,8E+6
12	1	2021	5,72E+6	1877588326	2,97E+10	0,55	106,4	0,940	1,4E+06	50	15,61	1E+06	4,30E+06				25	8,7E+6
13	1	2022	5,20E+6	1704081159	3,14E+10	0,58	99,3	0,942	1,3E+06	45	13,55	1E+06	3,90E+06				25	7,7E+6
14	1	2023	4,72E+6	1548673045	3,29E+10	0,61	92,7	0,945	1,2E+06	41	11,88	1E+06	3,54E+06				25	6,9E+6
15	1	2024	4,28E+6	1405476361	3,43E+10	0,63	86,8	0,947	1,1E+06	38	11,47	1E+06	3,22E+06				25	6,2E+6
16	1	2025	3,89E+6	1277192983	3,56E+10	0,66	81,4	0,949	9,7E+05	35	11,31	1E+06	2,92E+06				25	5,5E+6
17	1	2026	3,56E+6	1166335015	3,68E+10	0,68	76,5	0,951	8,9E+05	32	10,41	9E+05	2,67E+06				25	4,99E+6